

# Journal Pre-proof

Human macrophage migration inhibitory factor potentiates mesenchymal stromal cell efficacy in a clinically relevant model of allergic asthma

Ian J. Hawthorne, Hazel Dunbar, Courtney Tunstead, Tamara Schorpp, Daniel J. Weiss, Sara Rolandsson Enes, Claudia C. dos Santos, Michelle E. Armstrong, Seamas C. Donnelly, Karen English

PII: S1525-0016(23)00500-2

DOI: <https://doi.org/10.1016/j.ymthe.2023.09.013>

Reference: YMTHE 6192

To appear in: *Molecular Therapy*

Received Date: 5 July 2023

Accepted Date: 14 September 2023

Please cite this article as: Hawthorne IJ, Dunbar H, Tunstead C, Schorpp T, Weiss DJ, Enes SR, dos Santos CC, Armstrong ME, Donnelly SC, English K, Human macrophage migration inhibitory factor potentiates mesenchymal stromal cell efficacy in a clinically relevant model of allergic asthma, *Molecular Therapy* (2023), doi: <https://doi.org/10.1016/j.ymthe.2023.09.013>.

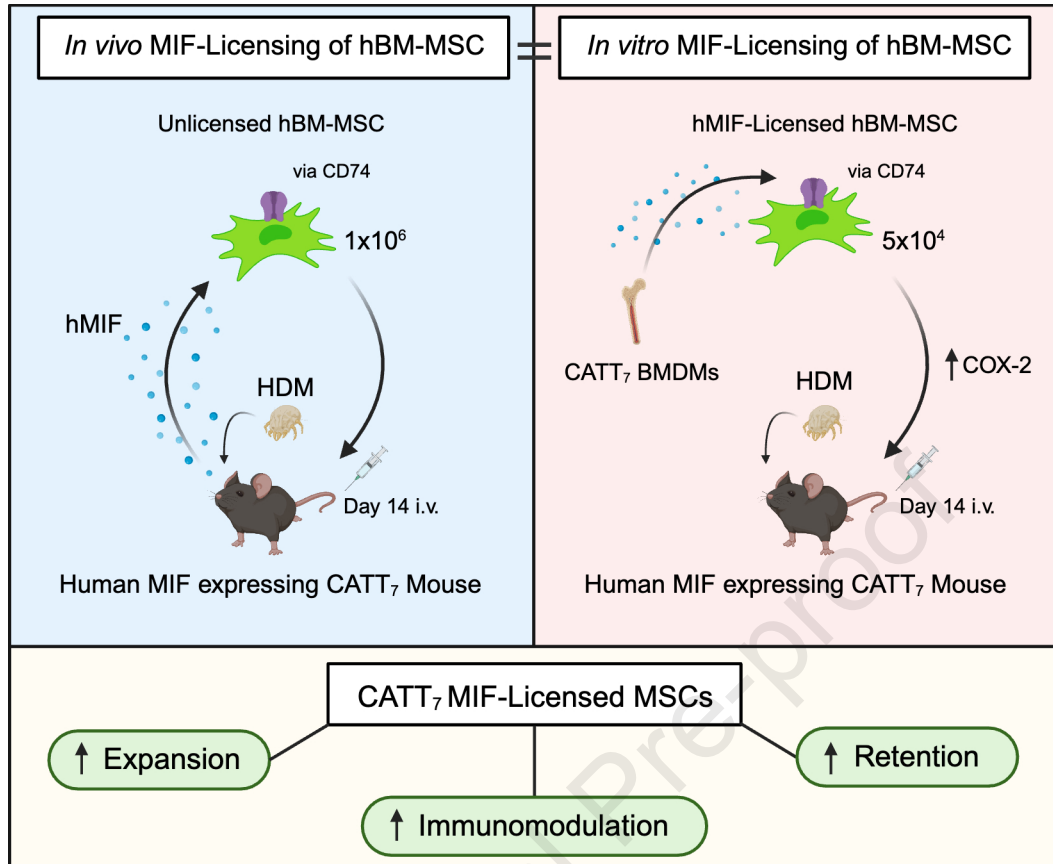
This is a PDF file of an article that has undergone enhancements after acceptance, such as the addition of a cover page and metadata, and formatting for readability, but it is not yet the definitive version of record. This version will undergo additional copyediting, typesetting and review before it is published in its final form, but we are providing this version to give early visibility of the article. Please note that, during the production process, errors may be discovered which could affect the content, and all legal disclaimers that apply to the journal pertain.

© 2023 The Author(s).



English and colleagues discuss how mesenchymal stromal cells significantly attenuated house dust mite-induced airway inflammation and airway remodelling in high MIF expressing CATT<sub>7</sub> mice. Blockade of CD74 or COX-2 function in MSCs prior to administration attenuated the efficacy of MIF-licensed MSCs *in vivo*.

Journal Pre-proof



1 **Human macrophage migration inhibitory factor potentiates mesenchymal stromal cell**  
2 **efficacy in a clinically relevant model of allergic asthma**

3 Ian J. Hawthorne<sup>1, 2, §</sup>, Hazel Dunbar<sup>1, 2, §</sup>, Courtney Tunstead<sup>1, 2</sup>, Tamara Schorpp<sup>1, 2</sup>, Daniel  
4 J. Weiss<sup>3</sup>, Sara Rolandsson Enes<sup>4</sup>, Claudia C. dos Santos<sup>5</sup>, Michelle E. Armstrong<sup>6</sup>, Seamas C.  
5 Donnelly<sup>6</sup>, Karen English<sup>1, 2\*</sup>

6 1. Kathleen Lonsdale Institute for Human Health Research, Maynooth University, Maynooth,  
7 Co. Kildare, Ireland

8 2. Department of Biology, Maynooth University, Maynooth, Co. Kildare, Ireland.

9 3. Department of Medicine, 226 Health Sciences Research Facility, Larner College of  
10 Medicine, University of Vermont, Burlington, VT 05405, USA

11 4. Department of Experimental Medical Science, Faculty of Medicine, Lund University,  
12 22100 Lund, Sweden

13 5. The Keenan Research Centre for Biomedical Science of St. Michael's Hospital, 30 Bond  
14 Street, Toronto, ON, Canada. Institute of Medical Sciences and Interdepartmental Division of  
15 Critical Care, Faculty of Medicine, University of Toronto, Toronto, ON, Canada.

16 6. Department of Medicine, Trinity College Dublin and Tallaght University Hospital, Co.  
17 Dublin, Ireland

18

19 <sup>§</sup> Denotes joint first authors.

20 **Running head:**

21 **MIF enhances MSC efficacy in asthma**

22 Corresponding Author Details:

23 \*Karen English, PhD.

24 Kathleen Lonsdale Institute for Human Health Research, Department of Biology, Maynooth  
25 University, Maynooth, Co. Kildare, Ireland.

26 Tel: +353-1-708-6290. Fax: +353-1-708-6337. Email: karen.english@mu.ie

27

28

29

30

31 **Abstract**

32 Current asthma therapies focus on reducing symptoms but fail to restore existing structural  
33 damage. Mesenchymal stromal cell (MSC) administration can ameliorate airway inflammation  
34 and reverse airway remodelling. However, differences in patient disease microenvironments  
35 seem to influence MSC therapeutic effects. Polymorphic CATT tetranucleotide repeat at  
36 position 794 of the human macrophage migration inhibitory factor (hMIF) gene has been  
37 associated with increased susceptibility and severity of asthma. We investigated the efficacy  
38 of human MSCs in high vs low hMIF environments and the impact of MIF pre-licensing of  
39 MSCs using humanised MIF mice in a clinically relevant house dust mite (HDM) model of  
40 allergic asthma. MSCs significantly attenuated airway inflammation and airway remodelling  
41 in high MIF expressing CATT<sub>7</sub> mice, but not in CATT<sub>5</sub> or wildtype littermates. Differences in  
42 efficacy correlated with increased MSC retention in the lungs of CATT<sub>7</sub> mice. MIF licensing  
43 potentiated MSC anti-inflammatory effects at a previously ineffective dose. Mechanistically,  
44 MIF binding to CD74 expressed on MSCs leads to upregulation of COX-2 expression.  
45 Blockade of CD74 or COX-2 function in MSCs prior to administration attenuated the efficacy  
46 of MIF-licensed MSCs *in vivo*. These findings suggest that MSC administration may be more  
47 efficacious in severe asthma patients with high MIF genotypes (CATT<sub>6/7/8</sub>).

48

## 49 Introduction

50 Allergic asthma is characterised by chronic airway inflammation and airway remodelling  
51 which refers to the structural changes in the airways. Currently, there is a heavy reliance on  
52 inhaled corticosteroids and long acting  $\beta$ 2-adenoreceptor agonists in the treatment of allergic  
53 asthma. The recent introduction of novel biologics such as benralizumab and dupilumab  
54 targeting Th2 cytokine receptors and tezepelumab targeting the alarmin thymic stromal  
55 lymphopoietin (TSLP) have been shown to significantly reduce allergic airway inflammation  
56 leading to reduced exacerbations and improved FEV<sub>1</sub> values.<sup>1,4</sup> However, not all patients are  
57 responders, and evidence for biologics to reverse existing airway remodelling in patients is thus  
58 far limited.<sup>5</sup> Thus, there is scope for novel therapeutics with capacity to attenuate inflammation  
59 and reverse remodelling to address the pitfalls in the current treatment and management of  
60 allergic asthma.

61 Mesenchymal stromal cells (MSCs) have immunomodulatory and anti-fibrotic properties and  
62 have proven therapeutic effects in a range of allergic airway inflammation models and are  
63 currently under investigation in two clinical trials for asthma ([NCT05147688](#), [NCT05035862](#)).  
64 Administration of MSCs intratracheally or intravenously has been shown to be effective in  
65 reducing airway inflammation and airway hyperresponsiveness in ovalbumin (OVA),<sup>6-17</sup>  
66 HDM,<sup>18-24</sup> and aspergillus hyphal extract<sup>25,26</sup> models. However, other studies fail to  
67 demonstrate efficacy in experimental asthma models.<sup>7,14,23,24,27,28</sup> To understand the  
68 mechanisms involved and to make MSCs a viable therapeutic in the clinic more focussed  
69 translational work is needed.

70 Under basal conditions, for example in healthy animals or individuals, MSC administration  
71 does not seem to alter immunological status or function (homeostasis is preserved). MSCs only  
72 become licensed to an anti-inflammatory phenotype in the presence of extrinsic factors.<sup>29</sup> Once  
73 licensed, MSCs modulate their surrounding microenvironment.<sup>30</sup> Importantly, their therapeutic  
74 effect is blunted in the presence of IFN $\gamma$ , NF- $\kappa$ B or TNF $\alpha$  receptor blockade/inhibition.<sup>31-33</sup>  
75 Moreover, in the absence of appropriate signals to license anti-inflammatory functions, MSCs  
76 may even exacerbate disease.<sup>34-36</sup> Licensing has been shown to improve MSC therapeutic  
77 efficacy by activating MSC anti-inflammatory characteristics prior to administration.  
78 Licensing through exposure to hypoxia,<sup>37,38</sup> inflammatory cytokines,<sup>39,40</sup> and pharmacological  
79 factors<sup>41</sup> have all been shown to improve MSC efficacy in a range of inflammatory diseases.  
80 Moreover, licensing of MSCs with serum from HDM-challenged mice<sup>18</sup> or with serum from

81 ARDS patients<sup>42</sup> enhanced MSC therapeutic efficacy *in vivo* in pre-clinical lung disease  
82 models. However, there are also *in vitro* studies reporting differential and in some cases  
83 negative effects of patient samples (acute respiratory distress syndrome (ARDS) versus cystic  
84 fibrosis (CF)) on MSC survival and function.<sup>42-44</sup>

85 Macrophage migration inhibitory factor (MIF) is an important regulator of host inflammatory  
86 responses demonstrated through its ability to promote the production of other inflammatory  
87 mediators. For example, MIF has been shown to amplify the expression of TNF, IFN $\gamma$ , IL-1 $\beta$ ,  
88 IL-2, IL-6 and IL-8 from immune cells.<sup>45-48</sup> This augmentation of immune signals contributes  
89 to MIF-mediated pathogenesis by acting to sustain inflammatory responses. This has been  
90 shown in a range of inflammatory diseases where the absence of MIF is associated with lower  
91 levels of pro-inflammatory cytokines resulting in reduced pathology. For example, MIF  
92 knockout (MIF<sup>-/-</sup>) mice display a less severe phenotype when exposed to OVA compared to  
93 control mice<sup>49-52</sup> and the use of anti-MIF antibodies or small molecule inhibitor (ISO-1) results  
94 in reduced Th2 cytokines in models of allergic airway inflammation.<sup>51,53-56</sup> High levels of MIF  
95 as a result of longer CATT repeats such as CATT<sub>7</sub> have been shown to increase severity in a  
96 range of diseases including severe anaemia (57), pneumococcal meningitis,<sup>58</sup> multiple  
97 sclerosis,<sup>59</sup> tuberculosis,<sup>60</sup> and COVID-19.<sup>61</sup> Importantly, associations between the CATT  
98 polymorphism and asthma incidence and severity have been observed.<sup>52</sup> Not only do these  
99 studies show the pivotal role that MIF plays in pro-inflammatory diseases they also affirm the  
100 importance of differences in the MIF CATT polymorphism.

101 Our previous work established a dominant role for MIF allelic variants in the severity of HDM-  
102 induced allergic asthma.<sup>62</sup> Using humanised high-expressing and low-expressing MIF mice in  
103 a HDM model of allergic airway inflammation we demonstrated the pivotal role MIF plays in  
104 exacerbating asthma pathogenesis. High levels of human MIF resulted in a significant increase  
105 in airway inflammation as a result of elevated levels of Th2 cytokines promoting infiltration of  
106 eosinophils into the airways. Furthermore, high levels of MIF were associated with airway  
107 remodelling with significant mucus hyperplasia, subepithelial collagen deposition, and airway  
108 hyperresponsiveness generating a more severe asthma phenotype. MIF has been shown to  
109 promote MSC migration *in vitro*,<sup>63</sup> however, the effect of MIF on MSC immunosuppressive  
110 function or therapeutic efficacy *in vivo* is unknown. Here, we sought to investigate the  
111 relationship between MIF and MSCs *in vivo* and to define conditions for optimal MSC  
112 therapeutic efficacy. The high MIF expressing CATT<sub>7</sub>, low MIF expressing CATT<sub>5</sub>, and WT

113 mice were used as a platform to investigate the role of MIF on MSC efficacy in a clinically  
114 relevant HDM-induced mouse model of allergic airway inflammation.

115

## 116 **Results**

### 117 **Human BM-MSCs significantly reduce airway remodelling in CATT<sub>7</sub> mice challenged** 118 **with HDM**

119 Firstly, to investigate the impact of high- and low-expressing MIF alleles on MSC treatment of  
120 allergic airway inflammation we examined the lung histology. CATT<sub>7</sub>, CATT<sub>5</sub>, and WT were  
121 randomized to HDM or mock (saline) intranasally 3 times a week for 3 weeks. Mice were then  
122 further randomized to 1x10<sup>6</sup> human BM-MSCs or equal volume saline administered via tail  
123 vein injection on day 14. On day 21, lung tissue was removed, formalin fixed and sectioned  
124 onto slides (Figure 1A). Slides were stained with PAS to highlight mucin production to assess  
125 the level of goblet cell hyperplasia. CATT<sub>7</sub> mice exhibit significantly higher levels of goblet  
126 cell hyperplasia compared to WT and CATT<sub>5</sub> mice. Administration of BM-MSCs reduced the  
127 level of goblet cell hyperplasia in all groups to almost background levels, with a significant  
128 reduction in the number of mucin secreting cells in the airways of HDM challenged CATT<sub>7</sub>  
129 mice (Figure 1B, 1C).

130 Subepithelial fibrosis was significantly increased in HDM challenged CATT<sub>7</sub> mice compared  
131 to the lower MIF expressing CATT<sub>5</sub> and WT groups. BM-MSC administration reduced the  
132 level of subepithelial fibrosis to almost background levels in all groups with significantly  
133 reduced subepithelial collagen deposition in HDM challenged CATT<sub>7</sub> mice (Figure 1D, 1E).  
134 In CATT<sub>5</sub> and WT mice challenged with HDM, BM-MSC administration had a small but not  
135 significant therapeutic effect. BM-MSC administration significantly mitigated increased  
136 inflammatory infiltrate and H&E pathological score in CATT<sub>7</sub> mice challenged with HDM  
137 (Figure S1).

### 138 **Human BM-MSCs significantly reduce airway inflammation in CATT<sub>7</sub> mice challenged** 139 **with HDM**

140 Total cell counts were significantly elevated in the BAL fluid of CATT<sub>7</sub> mice following HDM  
141 challenge (Figure 2A). MSCs significantly reduced the number of total infiltrating cells in the



142 BALF of CATT<sub>7</sub> mice (Figure 2A). Differential cell counts identified eosinophils as the main  
143 cell infiltrating into the lung tissue following HDM challenge and MSCs significantly  
144 decreased infiltrating eosinophils in CATT<sub>7</sub> mice yet had no effect in the CATT<sub>5</sub> and WT  
145 groups (Figure 2B). IL-4 and IL-13 were significantly elevated in the BAL fluid of CATT<sub>7</sub>  
146 mice following HDM challenge (Figure 2C, 2D). These Th2 cytokines are not significantly  
147 upregulated in CATT<sub>5</sub> or WT mice. While MSCs significantly decreased IL-4 and IL-13 in  
148 CATT<sub>7</sub> mice, MSC treatment did not reduce and in some cases increased Th2 cytokines in the  
149 BAL fluid of CATT<sub>5</sub> and WT mice (Figure 2C, 2D). These data show that BM-MSCs are  
150 effective at alleviating eosinophil infiltration and reducing Th2 cytokines in a high MIF  
151 expressing model of allergic asthma and that MSCs require a threshold level of inflammation  
152 to mediate their therapeutic effects.

### 153 **High levels of hMIF significantly enhance BM-MSc retention in a HDM model of allergic** 154 **asthma**

155 Next, we analysed the biodistribution of MSCs following administration into HDM challenged  
156 WT, CATT<sub>5</sub> and CATT<sub>7</sub> mice.  $1 \times 10^6$  fluorescently labelled BM-MSCs were administered i.v.  
157 via tail vein injection on day 14. On day 15 mice were sacrificed and the lungs prepared for  
158 CryoViz imaging (Figure 3A-C). Significantly higher numbers of labelled MSCs were detected  
159 in the lung of high MIF expressing CATT<sub>7</sub> mice compared to the low expressing CATT<sub>5</sub> or  
160 WT littermate control (Figure 3C, 3D). However, the number of clusters of labelled BM-MSCs  
161 within the lungs remained unchanged among the groups (Figure 3E). Taken together, these  
162 data suggest prolonged MSC-pulmonary retention time increases the number of MSCs retained  
163 at the site of inflammation 24 hr post administration. These data suggest that high levels of  
164 MIF may provide a longer window for MSCs to carry out their therapeutic effects.

### 165 **The influence of MIF on MSC expression of immunomodulatory factors and MSC** 166 **cytokine licensing *in vitro***

167 MSCs mediate their therapeutic effects via expression or production of secreted factors *in vitro*  
168 and *in vivo*<sup>64</sup> and licensing with proinflammatory cytokines such as IFN $\gamma$  or TNF $\alpha$ <sup>65-69</sup> can  
169 enhance expression of immunomodulatory mediators. Here, we characterised the effect of  
170 recombinant human MIF on the expression of IDO, COX-2, PTGES, ICAM-1 and HGF in  
171 untreated MSCs or MSCs licensed with IFN $\gamma$  or TNF $\alpha$ . rhMIF (1ng/ml) stimulation alone did  
172 not increase expression of IDO, COX-2, PTGES, ICAM-1 or HGF (Figure 4A-E) in human

173 BM-MSCs. Following licensing with TNF $\alpha$ , MIF stimulation enhanced MSC expression of  
174 COX-2 and PTGES (Figure 4B-C). In IFN $\gamma$  licensed MSCs, rhMIF stimulation did not enhance  
175 MSC expression of IDO or HGF and significantly reduced ICAM-1 expression (Figure 4A,  
176 4D, 4E). We confirmed these findings at the protein level for IDO and COX-2 using  
177 intracellular flow cytometry (Figure 4F-G). Using increasing doses of rhMIF (1, 10 or 100  
178 ng/ml), we showed that COX-2 expression is increased in a dose-dependent manner by rhMIF  
179 stimulation in TNF $\alpha$  licensed MSCs, with COX-2 expression plateauing at 10ng/ml of rhMIF  
180 (Figure 4H). The MIF receptor CD74 is expressed by MSCs, however, rhMIF stimulation (dose  
181 range 1, 10 or 100ng/ml) does not enhance CD74 expression (Figure 4I).

### 182 **CATT<sub>7</sub> MIF licensing enhances MSC expansion and immunosuppressive function *in vitro***

183 In order to investigate the effect of endogenous MIF from CATT<sub>7</sub> mice on MSC expression of  
184 immunomodulatory factors, we generated bone marrow-derived macrophages (BMDMs) from  
185 CATT<sub>7</sub> mice and used the conditioned medium (CM) as a source of endogenous human MIF  
186 (Figure 5A) to license MSCs. The concentration of human MIF in CATT<sub>7</sub> BMDM CM ranged  
187 from ~3000–4000 pg/ml (Figure S2).

188 MIF may have a negative role in the regulation of IDO expression as MIF<sup>-/-</sup> mice produce more  
189 IDO,<sup>70</sup> however, MIF has an established role as an upstream positive regulator of  
190 cyclooxygenase 2 (COX-2) through the activation of the MAPK signalling pathway.<sup>71,72</sup> IDO,  
191 COX-2 and PGE2 are widely reported mediators of MSC immunosuppression.<sup>39,73</sup> MSCs  
192 constitutively express COX-2 but not IDO. IFN $\gamma$  licensing of MSCs leads to expression of IDO  
193 while TNF $\alpha$  enhances MSC COX-2 expression.<sup>68</sup> Here we show that CATT<sub>7</sub> MIF stimulation  
194 reduces MSC IDO production (Figure 5B-C), however, the percentage of COX-2 expressing  
195 MSCs was significantly increased following CATT<sub>7</sub> MIF stimulation (Figure 5D-E). Human  
196 MSCs express the MIF receptor CD74 and this expression is maintained and not increased  
197 following exposure to CATT<sub>7</sub> MIF CM (Figure 5F). In line with other studies,<sup>74</sup> we show that  
198 IFN $\gamma$  stimulation leads to significantly increased MSC CD74 expression and CATT<sub>7</sub> MIF CM  
199 does not significantly alter that (Figure 5F). This aligns with our data showing that MIF does  
200 not enhance IFN $\gamma$  regulated IDO expression. Given the potentiating effect of MIF on the TNF $\alpha$   
201 regulated gene COX-2 in MSCs, we examined the influence of CATT<sub>7</sub> MIF on MSC  
202 expression of the TNF $\alpha$  regulated genes TSG-6 and PTGS2. The presence of CATT<sub>7</sub> MIF CM  
203 significantly reduced TSG-6 in TNF $\alpha$  stimulated MSCs (Figure 5G), but did not significantly

204 alter the expression of PTGS2 (Figure 5H). MSCs licensed with high levels of hMIF from  
205 CATT<sub>7</sub> CM displayed enhanced suppression of T cell proliferation compared to the untreated  
206 MSCs, however this was not statistically significant in the frequency of proliferating CD3<sup>+</sup> T  
207 cells (Figure 5I) or the number of proliferating CD3<sup>+</sup> T cells (Figure 5J). The presence of SCD-  
208 19 abrogated the enhanced suppression mediated by hMIF licensed MSCs, as the number of  
209 proliferating CD3<sup>+</sup> T cells was significantly increased compared to the CATT<sub>7</sub>MSC group  
210 (Figure 5J).

211 Previous studies have shown that MIF has the ability to support cell proliferation *in vitro*.<sup>75-77</sup>  
212 Increasing the number of MSCs within the inflammatory niche could prove to be important in  
213 enhancing MSC immunoregulatory effects. High levels of MIF significantly enhanced MSC  
214 expansion *in vitro* compared to the complete medium control group (Figure 5K). Blockade of  
215 MIF using SCD-19 confirmed the role of MIF in driving MSC expansion (Figure 5K). This  
216 data might help to explain the enhanced retention of MSCs in CATT<sub>7</sub> HDM challenged mice  
217 (Figure 3) but further experiments would be required to confirm that.

#### 218 **Titration of BM-MSc doses in CATT<sub>7</sub> mice challenged with HDM**

219 Next, we investigated if MIF licensing could improve MSC efficacy in the high MIF expressing  
220 CATT<sub>7</sub> mice challenged with HDM. To do this we first investigated the dose at which MSCs  
221 lose efficacy. MSCs at doses of 1x10<sup>6</sup>, 5x10<sup>5</sup>, 1x10<sup>5</sup>, and 5x10<sup>4</sup> were administered i.v. into  
222 HDM challenged CATT<sub>7</sub> on day 14 (Figure 6A). MSCs maintained efficacy as low as 1x10<sup>5</sup>  
223 cells with reduced immune cell infiltration (Fig. 6B, 6C) and reduced Th2 cytokines IL-4  
224 (Figure 6D) and IL-13 (Figure 6E). We observed that BM-MSCs were no longer able to carry  
225 out their immunosuppressive effects at a dose of 5x10<sup>4</sup>. At 5x10<sup>4</sup> BM-MSCs were unable to  
226 reduce the number of eosinophils infiltrating into the lungs (Figure 6B, 6C) or regulate Th2  
227 cytokine production (Figure 6D, 6E).

#### 228 **MIF licensing restores MSC efficacy at low doses in CATT<sub>7</sub> mice**

229 To investigate the effect of MIF licensing on MSC therapeutic efficacy MSCs were first  
230 licensed *in vitro* by stimulation with bone marrow-derived macrophage (BMDM) conditioned  
231 media from CATT<sub>7</sub> or KO mice for 24 hr. 5x10<sup>4</sup> MSCs, MIF licensed MSCs (CATT<sub>7</sub>MSC), or  
232 MIF KO licensed MSCs (K<sup>O</sup>MSC) were administered i.v. into CATT<sub>7</sub> mice via tail vein  
233 injection on day 14 in HDM challenged mice. On day 18, BAL fluid was collected, cell counts  
234 were performed and Th2 cytokines were measured (Figure 7A). Only CATT<sub>7</sub>MSC administration

235 significantly reduced total cell counts and number of eosinophils in CATT<sub>7</sub> mice challenged  
236 with HDM (Figure 7B, 7C). CATT<sub>7</sub>MSCs markedly reduced IL-4 and IL-13 levels compared to  
237 control group although not significantly (Figure 7D, 7E). The control MSC group and the  
238 K<sup>0</sup>MSC group displayed similar levels of immune cell infiltration and Th2 cytokine production  
239 suggesting the effects observed in the CATT<sub>7</sub>MSC group are specific to MIF licensed MSCs.  
240 These data show that MIF licensing can restore MSC immunosuppressive function at doses  
241 that would normally be ineffective.

#### 242 **Blocking COX-2 abrogates therapeutic efficacy of MIF licensed BM-MSCs**

243 COX-2 is the rate-limiting enzyme involved in the synthesis of arachidonic acid to PGE<sub>2</sub>, a  
244 key mediator in the immunomodulatory effects of MSCs.<sup>78</sup> To assess the role of COX-2 on  
245 MIF licensed MSCs we inhibited COX-2 with indomethacin. MSCs were treated with  
246 indomethacin (10 µM) for 30 min. Following the 30 min pre-treatment, cells were incubated  
247 with CATT<sub>7</sub> CM for 24 hours. To further validate the involvement of MIF in the improvement  
248 of MSC efficacy, MSCs were exposed to an anti-CD74 neutralising antibody (10 µg/ml) or  
249 IgG1 isotype control (10 µg/ml) for 30 min. MSCs were then incubated with CATT<sub>7</sub> CM for  
250 24 hours (Figure 8A). Analysis of the BAL fluid cell counts showed that pre-treating MSCs  
251 with indomethacin before administration significantly reduces CATT<sub>7</sub>MSCs ability to suppress  
252 immune cell infiltration in the BAL fluid of CATT<sub>7</sub> mice challenged with HDM (Figure 8B,  
253 8C). Additionally, the analysis of the Th2 cytokines in the BALF showed a marked increase in  
254 IL-4 (Figure 8D) and a significant increase in the levels of IL-13 (Figure 8E) in the  
255 indomethacin group compared to the control MIF licensed MSC group. Taken together, these  
256 results show that COX-2 is an important mediator in the enhancement of therapeutic efficacy  
257 associated with MIF licensing. Furthermore, blocking of CD74 abrogates MIF licensed BM-  
258 MSC suppression of eosinophil infiltration and type 2 cytokines in the BAL (Figure 8). These  
259 data indicate that MIF enhances MSCs' immunomodulatory capacity mainly through CD74  
260 signalling to upregulate COX-2 production.

261

#### 262 **Discussion**

263 Our main results advance the field of MSC-based therapeutics for asthma by demonstrating  
264 that (i) MSC treatment is highly effective in ameliorating airway inflammation; (ii) their

265 therapeutic potential can be enhanced by MSC-MIF licensing as demonstrated in high MIF  
266 expressing CATT<sub>7</sub> mice; and finally (iii) that the mechanism of MIF-licensing is dependent  
267 upon MSC-CD74 expression levels that drive COX-2 expression in MSCs. Our data aligns  
268 with the literature demonstrating the ability of human MSCs to ameliorate eosinophil  
269 infiltration by reducing the levels of Th2 cytokines.<sup>8,10-12,25,79</sup> In addition to reducing  
270 inflammation, MSCs also alleviate features of airway remodelling in the CATT<sub>7</sub> mice.  
271 Interestingly while MSCs were effective at reducing the severity of goblet cell hyperplasia and  
272 subepithelial fibrosis in all groups, we did not observe the same changes in type 2 inflammatory  
273 markers in the BAL of WT and low MIF expressing CATT<sub>5</sub> mice suggesting that high levels  
274 of MIF may be responsible for improving MSC efficacy. The reduced efficacy of MSCs in the  
275 WT and CATT<sub>5</sub> mice is likely attributed to lack of inflammation present associated with a bias  
276 towards Th1 immunity in C57BL/6 mice compared to the more Th2 bias in BALB/c mice,  
277 influencing the level of Th2 response in our HDM challenge model.<sup>80</sup> There have been several  
278 instances where researchers also observed poor responses to MSC treatment of allergic airway  
279 inflammation in C57BL/6 mice.<sup>7,23</sup> More recently, Castro et al. report the requirement of at  
280 least 2 doses of human AD-MSCs to reverse airway remodelling and alleviate inflammation in  
281 HDM challenged C57BL/6 mice.<sup>21</sup>

282 We show that a single human MSC dose is capable of significantly decreasing airway  
283 remodelling in CATT<sub>7</sub> mice. This suggests that high levels of MIF may facilitate activation of  
284 MSCs improving their therapeutic efficacy and leading to reversal of airway remodelling. The  
285 literature surrounding MSC's effect on airway remodelling is conflicting, however, the  
286 majority of the current literature demonstrates that MSCs can attenuate airway  
287 remodelling.<sup>8,10,14,15,17,18,28</sup> Others report a deficit in MSCs capacity to ameliorate goblet cell  
288 hyperplasia<sup>14,19,23</sup> or subepithelial collagen deposition.<sup>9,28</sup> Reasons for these discrepancies  
289 include source of MSCs,<sup>8,23,81</sup> genotypic mouse model differences, severity of mouse models,  
290 time of infusion, MSC fitness, dosing, and route of administration.<sup>27</sup>

291 Our previous studies have demonstrated that pro-inflammatory cytokine licensing of MSCs or  
292 MSC-like cells; multipotent adult progenitor cells (MAPCs) enhances their retention in  
293 inflammatory conditions and correlates with enhanced therapeutic efficacy.<sup>39,82</sup> We detected  
294 significantly higher numbers of MSCs in the lungs of HDM challenged CATT<sub>7</sub> mice compared  
295 to CATT<sub>5</sub> or littermate controls 24 hours following administration. It is suggested that short-  
296 term effects of MSCs are mediated by their diverse secretome and the longer-term effects of

297 MSC therapy are a result of direct interaction with other cell types.<sup>83</sup> Increased longevity at the  
298 site of injury allows MSCs a longer period to secrete soluble factors and interact with cells in  
299 the inflammatory microenvironment. MSC retention in the CATT<sub>7</sub> HDM challenged mice is  
300 an important observation and future work will determine if enhanced retention is also involved  
301 in the enhanced MSC efficacy observed.

302 Taken together these data suggest that MSCs are more efficacious in the high MIF environment  
303 of CATT<sub>7</sub> mice. By investigating the effects of different concentrations of a human cytokine  
304 on the efficacy of human MSCs in a model of allergic asthma using a clinically relevant  
305 allergen, we have identified a specific disease microenvironment which supports and enhances  
306 MSC efficacy. The use of our humanised model aims to provide a more accurate depiction of  
307 how human MSCs would interact in subsets of patients compared to conventional murine  
308 models. Of course, despite exploring the effect of a human cytokine on human MSCs there are  
309 still limitations as we are unable to fully mimic clinical severe allergic asthma and the use of  
310 transgenic MIF mice on a C57BL/6 background meant that control WT mice do not develop a  
311 high level of type 2 inflammation. However, these results may have implications in tailoring  
312 MSC treatment in cases of severe asthma. Our results have demonstrated that MSCs are less  
313 efficacious in low MIF environments. Patients with 5/5 haplotypes tend to have lower levels  
314 of circulating MIF<sup>84</sup> and therefore may not respond as well to MSC treatment. Whereas patients  
315 with 6/6, 7/7 or 8/8 haplotypes are more likely to have high levels of circulating MIF<sup>52,85,86</sup>  
316 which may lead to greater MSC activation and enhanced therapeutic efficacy.

317 Following on from the discovery that MSC administration into CATT<sub>7</sub> mice led to improved  
318 MSC efficacy, we investigated strategies to use the high MIF microenvironments to potentiate  
319 the effects of MSCs. Past work in our lab has focussed on different licensing strategies of MSCs  
320 to enhance MSC efficacy. Previously, we have demonstrated how IFN $\gamma$  licensing can improve  
321 MSC efficacy in a humanised model of acute GvHD and how endogenous factors such as  
322 peroxisome proliferator-activated receptor (PPAR) $\delta$  ligands or treatments like cyclosporine A  
323 can influence this.<sup>39,40</sup> Other studies have shown how licensing with pharmacological agents  
324 or endogenous factors can further enhance the effects of MSC therapy in preclinical models of  
325 asthma.<sup>18,19,87</sup>

326 One of the main criticisms of preclinical research is the use of doses which far exceed what  
327 would be reasonable in the clinic. Analysis of clinical trials using i.v. injection of MSCs reveals  
328 that the minimal effective dose used ranges from 1-2 million cells/kg.<sup>88</sup> Studies which have

329 investigated the i.v. administration of MSCs in preclinical models of allergic asthma administer  
330 doses which equate to 4-40 million cells/kg with the majority at the higher end of the  
331 scale.<sup>8,10,12,16,20-22,25,26,28,79,89-92</sup> The efficacy observed with MIF licensed MSCs using  $5 \times 10^4$   
332 cells per mouse results in an effective dose of 2 million cells/kg. This shows that through MIF  
333 licensing we are able to restore MSC efficacy at a dose akin to what is used in clinical trials.

334 We then sought to elucidate the mechanisms involved. Given our use of human MSCs in a  
335 mouse host, the interspecies ligand/receptor non-functionality can raise questions about how  
336 human MSCs might mediate their effects in a mouse host. We and others have shown that  
337 indeed human MSCs can mediate protective effects in mouse hosts.<sup>8,10-12,14-17,21,24,25,33,93</sup> Four  
338 studies have tracked human MSC biodistribution following i.v. administration in patients with  
339 COPD,<sup>94</sup> liver cirrhosis,<sup>95</sup> haemophilia A<sup>96</sup> or breast cancer.<sup>97</sup> No MSCs were detected in blood  
340 at 1hr post infusion. MSCs were distributed mainly in the lung<sup>95</sup> or lungs and liver<sup>96</sup> at 48 hr  
341 post i.v. infusion with the signal decreasing thereafter. As such, these studies suggest that  
342 biodistribution of human MSCs following i.v. administration in humans aligns with the studies  
343 investigating MSC biodistribution in mouse models.<sup>98</sup>

344 In terms of mechanism, MIF mediated signal transduction is primarily initiated by binding to  
345 MIF's classical receptor CD74.<sup>99</sup> We showed that blocking CD74 on the surface of MSCs  
346 ultimately abolished their immunosuppressive abilities. These findings not only reaffirmed that  
347 the licensing with CATT<sub>7</sub> CM was MIF mediated but it also showed that these effects were  
348 dependent on binding to CD74. MIF signal transduction through CD74 binding has been shown  
349 to initiate a range of signalling pathways which induce cell proliferation, resistance to  
350 apoptosis, and the promotion of repair.<sup>100-104</sup> Furthermore, MIF binding to CD74 has been  
351 shown to activate cytosolic phospholipase A2 (cPLA<sub>2</sub>). Moreover, cPLA<sub>2</sub> activation results in  
352 the mobilisation of arachidonic acid from membrane phospholipids which is a precursor to the  
353 synthesis of prostaglandins.<sup>105</sup> Interestingly MIF can upregulate COX-2 expression, a rate  
354 limiting step in the synthesis of prostaglandins such as PGE<sub>2</sub>,<sup>71,72,106</sup> however, MIF has been  
355 shown to have no effect on the expression of COX-1.<sup>71</sup>

356 The COX-2/PGE<sub>2</sub> pathway has been extensively documented as being one of the key mediators  
357 driving MSC immunomodulation.<sup>39,68,107,108</sup> Our data shows that MIF stimulation enhances the  
358 expression of COX-2 but not TSG-6 or PTGS2 in untreated and TNF $\alpha$  licensed MSCs. We  
359 hypothesised that the COX-2/PGE<sub>2</sub> pathway could be involved in the restoration of MSCs  
360 immunomodulatory capacity following CATT<sub>7</sub> licensing. To investigate, we pre-treated MSCs

361 with indomethacin prior to licensing. Indomethacin is a potent non-selective inhibitor of COX-  
362 1 and COX-2.<sup>109</sup> We showed that blocking COX-2 abrogated therapeutic efficacy of CATT<sub>7</sub>  
363 licensed MSCs. Interestingly we observed that blocking of COX-2 via indomethacin had more  
364 pronounced effect than blocking CD74. COX-2 is constitutively expressed in human MSCs,  
365 therefore, inhibition with indomethacin also blocks basal COX-2 expression which will  
366 contribute to the effects observed.

367 These data show that MIF licensing can improve MSC therapeutic efficacy through the  
368 upregulation of COX-2 which likely drives PGE<sub>2</sub> production. Our data agrees with several  
369 studies in the literature which also reveal the ability of MIF to improve MSC efficacy *in*  
370 *vivo*.<sup>110-112</sup> The Zhang group demonstrated the ability of MIF to improve MSC therapeutic  
371 efficacy by transducing MSCs with a lentiviral vector containing *Mif* cDNA thus promoting  
372 MIF overexpression.<sup>110-112</sup> Furthermore, Zhang et al. demonstrated the ability of MIF to  
373 upregulate COX-2 expression and promote PGE<sub>2</sub> production in astrocytes.<sup>113</sup> Here, we further  
374 demonstrate the effects of *ex vivo* MIF licensing on MSC therapeutic efficacy by showing  
375 binding to CD74 and increased COX-2 expression enhances MSCs immunomodulatory  
376 abilities.

377 The knowledge gained from this study can be used to further optimise MSCs as a therapy and  
378 provide a basis for future studies regarding the effects of MSCs on the immune response in  
379 high MIF environments such as in asthma patients exhibiting the CATT<sub>7</sub> polymorphism.

380

## 381 **Materials and Methods**

### 382 **Ethical Approval**

383 All procedures involving the use of animals or human materials were carried out by licensed  
384 personnel. Ethical approval for all work was granted by the biological research ethics  
385 committee of Maynooth University (BRESC-2018-013). Project authorization was received  
386 from the scientific animal protection unit of the health products regulatory agency (HPRA)  
387 under AE19124/P022 whereby the terms of the animal experiments within this project were  
388 outlined and adhered to in accordance with the ARRIVE criteria.



### 389 **Human bone marrow derived MSC culture**

390 Three different human bone marrow-derived MSC (BM-MSC) donors were obtained from  
391 RoosterBio Inc. (Frederick, MD, USA). MSCs were first expanded in RoosterBio proprietary  
392 expansion medium (RoosterBasal and RoosterBooster) for the first two passages according to  
393 manufacturer's instructions. Following this MSCs were cultured and maintained in Dulbecco's  
394 Modified Eagles Media Low Glucose (DMEM, Sigma-Aldrich, Arklow, Wicklow, Ireland)  
395 supplemented with 10% (v/v) foetal bovine serum (FBS) (BioSera, Cholet, France) and 1%  
396 (v/v) Penicillin/Streptomycin (Sigma-Aldrich). Human MSCs were seeded at  $1 \times 10^6$  cells per  
397 T175 flask and cultured at 37 °c in 5% CO<sub>2</sub>. Media was replenished every 2-3 days, and cells  
398 passaged once they achieved 80% confluency. All experiments were carried out between  
399 passages 2-5.

### 400 **MSC Characterisation**

401 Three different human bone marrow-derived MSC (BM-MSC) donors (identified as 001-177,  
402 003-307 and 003-310) from RoosterBio Inc. (Frederick, MD, USA) were characterised by  
403 analysing the expression of cell surface markers. All MSCs donors were found to be negative  
404 for CD34 (FITC), CD45 (APC) and HLA-DR (PE) and positive for CD73 (APC), CD90 (FITC)  
405 and CD105 (PE) (BD Pharmingen, San Diego, CA, USA) by the Attune Nxt Flow Cytometer  
406 (Figure S3).

### 407 **Animal Strains**

408 Two C57BL/6 mouse strains expressing the human high- or low-expression MIF alleles  
409 ( $MIF^{CATT7}$  [(C57BL/6NTac-Mif<sup>tm3884.1(MIF)Tac-Tg(CAG-Flpe)2Arte] and  $MIF^{CATT5}$   
410 [C57BL/6NTac-Mif<sup>tm3883.1(MIF)Tac-Tg(CAG-Flpe)2Arte] mice) were created using  
411 vector-based recombinant replacement of murine *Mif* by Taconic Biosciences (Rensselaer,  
412 NY) (Fig. 1). Validation of the expression of human and not murine *MIF* mRNA was verified  
413 by qPCR, and -794 CATT-length dependent stimulated MIF production was confirmed *in*  
414 *vivo*.<sup>61</sup> Littermate wildtype (WT) and  $MIF^{-/-}$  ( $MIF$  KO)<sup>114</sup> (a kind donation from R. Bucala,  
415 Yale School of Medicine, Yale University, New Haven, CT, USA) mice were used as controls.</sup></sup>

## 416 **HDM-induced Airway Inflammation Model and Therapeutic Protocol**

417 Both male and female MIF<sup>CATT7</sup>, MIF<sup>CATT5</sup> or WT mice aged 6-12 weeks were challenged with  
418 25 µg HDM extract (*Dermatophagoides pteronyssinus*, Greer Laboratories, Lenoir, NC, USA)  
419 in 25 µl phosphate buffered saline (PBS) intranasally (i.n.) 3 days weekly for 3 weeks under  
420 light isoflurane anaesthesia. Control mice were challenged with 25 µl PBS under the same  
421 conditions. On day 14, after HDM challenge, mice received an intravenous (i.v.) injection of  
422  $1 \times 10^6$  MSCs in 300 µl into the tail vein.<sup>115</sup> For the dose curve  $1 \times 10^6$ ,  $5 \times 10^5$ ,  $1 \times 10^5$ , and  $5 \times 10^4$   
423 were administered i.v. into HDM challenged CATT<sub>7</sub> mice on day 14.  $5 \times 10^4$  was selected as the  
424 dose at which MSCs lose efficacy.

## 425 **Licensing of MSCs with Endogenous Human MIF**

426 Supernatants containing endogenous human MIF were generated from bone marrow- derived  
427 macrophages (BMDMs) of C57BL/6 mouse strains expressing the high-expressing MIF allele  
428 (CATT<sub>7</sub>). CATT<sub>7</sub> mice were challenged with HDM in 25 µl phosphate buffered saline (PBS)  
429 intranasally 3 days weekly for 3 weeks under light isoflurane anaesthesia. 4 hr post final  
430 challenge, femurs and tibias were flushed with warm Roswell Park Memorial Institute (RPMI)  
431 1640 medium GlutaMAX<sup>TM</sup> (Gibco, Paisley, UK) supplemented with 10% (v/v) heat  
432 inactivated foetal bovine serum (FBS) (BioSera) and 1% (v/v) Penicillin/Streptomycin (Sigma-  
433 Aldrich). Cells were collected and seeded into T175 flasks in cRPMI supplemented with 10%  
434 L929 conditioned medium. L929 cell line produces high amounts of macrophage colony  
435 stimulating factor (M-CSF) and other proteins stimulating macrophage differentiation. After  
436 96 hours, supernatants were collected, sterile filtered (0.22 µm pore size) and stored at -20°C.  
437 The conditioned media generated in this manner will be referred to as CATT<sub>7</sub> CM.  
438 Additionally, KO CM was generated from MIF KO mice as a control. Licensing MSCs was  
439 performed by removing existing media, washing with PBS, and incubating cells with CATT<sub>7</sub>  
440 CM (<sup>CATT7</sup>MSC) or MIF KO CM (<sup>KO</sup>MSC) for 24 hr. To account for variability of human MIF  
441 levels between CATT<sub>7</sub> mice and to ensure WT mice did not produce human MIF, CATT<sub>7</sub>,  
442 CATT<sub>5</sub> and WT supernatants were measured by human MIF ELISA (R&D Systems, MN,  
443 USA) as described previously (Figure S2).<sup>62</sup>  $5 \times 10^4$  licensed MSCs were administered i.v. into  
444 HDM challenged CATT<sub>7</sub> mice on day 14. Where indicated, MSCs were treated with COX-2  
445 inhibitor indomethacin (10 µM) for 30 min. Following pre-treatment, MSCs were licensed with  
446 CATT<sub>7</sub> CM for 24 hr as described above. Moreover, mouse anti-CD74 neutralising antibody

447 and isotype control were added to the assay. MSCs were pre-treated with anti-CD74  
448 neutralising antibody (clone LN2) (10 µg/ml) or IgG1 κ isotype control (clone T8E5) (10  
449 µg/ml) for 30 min. MSCs were then licensed with CATT<sub>7</sub> CM for 24 hr before administration.

#### 450 **Collection of Bronchoalveolar Lavage (BAL) Fluid**

451 On day 18, 4 hr post final challenge, mice were sacrificed for cell and cytokine analysis of the  
452 BAL fluid. BAL fluid was obtained through 3 gentle aspirations of PBS. After centrifugation,  
453 protease inhibitor cocktail (Roche Diagnostics, Mannheim, Germany) was added to the  
454 supernatants before Th2 cytokine analysis. Total numbers of viable BAL cells were counted  
455 using ethidium bromide/acridine orange staining on a haemocytometer then pelleted onto  
456 microscope slides by cytocentrifugation. Slides were stained with Kwik Diff kit stain (Richard-  
457 Allan Scientific, Kalamazoo, MI, USA) and coverslips were mounted using DPX mounting  
458 medium (Sigma-Aldrich). Differential cells counts were derived by counting a minimum of  
459 300 leukocytes on randomly selected fields under a light microscope at 20X magnification.

#### 460 **Enzyme-linked immunosorbent assay (ELISA)**

461 Levels of mIL-4 (Biolegend, San Diego, CA, USA) and mIL-13 (eBioscience, San Diego, CA,  
462 USA) were determined using commercial ELISA kits, according to manufacturer's  
463 instructions.

#### 464 **Lung Histology**

465 On day 21, mice were sacrificed for histological analysis. Lungs were removed and fixed in  
466 10% neutral buffered formalin, paraffin embedded and 5 µm slices were mounted onto slides  
467 for histological analysis. Lung tissue was stained with haematoxylin and eosin (H&E), periodic  
468 acid-Schiff (PAS) or Masson's Trichrome to analyse immune cell infiltration, goblet cell  
469 hyperplasia or subepithelial collagen deposition respectively. H&E analysis was carried out as  
470 previously described.<sup>116</sup> Goblet cell hyperplasia was determined by the % of PAS positive cells  
471 in airways relative to airway diameter. Subepithelial collagen deposition was calculated by  
472 analysing the % of positive staining using the trainable Weka segmentation plugin on Fiji open-  
473 source software.

## 474 **Cryo-Imaging**

475  $1 \times 10^6$  MSCs were labelled with the Qtracker® 625 labelling kit (Invitrogen, Paisley, UK)  
476 according to manufacturer's instructions before being administered i.v. on day 14. On day 15,  
477 mice were humanely euthanised, and the lungs were embedded in mounting medium for  
478 cryotomy (O.C.T compound, VWR Chemicals, Leuven, Switzerland), frozen in liquid nitrogen  
479 and stored at  $-80^\circ\text{C}$ . Lungs were sectioned into  $40 \mu\text{m}$  slices and imaged with the automated  
480 CryoViz™ imaging system (BioInvision Inc., Cleveland, OH, USA). Images were then  
481 processed to generate 3D images using CryoViz™ processing, and the number of detected cells  
482 was quantified using cell detection software (BioInvision).<sup>39</sup>

## 483 **Analysis of Gene Expression**

484 Total RNA was extracted using TRIzol (Ambion Life Sciences, Cambridgeshire, UK)  
485 according to manufacturer's instructions. RNA concentrations were measured using a  
486 spectrophotometer (Nanodrop 2000, ThermoScientific, Wilmington DE, USA) and were  
487 equalised to  $100\text{ng}/\mu\text{l}$  before cDNA synthesis. cDNA synthesis was performed using  
488 manufacturer's instructions (Quantabio, MA, USA). Real Time-Polymerase Chain Reaction  
489 (RT-PCR) was carried out using PerfeCta SYBR Green FastMix (Quantbio, MA, USA).  
490 Expression of human COX-2, PTGES, IDO, ICAM-1, HGF, TSG-6 and PTGS2 (primer  
491 sequence information is contained in Table S1) was quantified in relation to the housekeeper  
492 gene HPRT using the  $\Delta\text{CT}$  method. The fold change in the relative gene expression was  
493 determined by calculating the  $2^{-\Delta\Delta\text{CT}}$  values.

## 494 **MSC Expansion Assay**

495  $1.4 \times 10^5$  MSCs were seeded out into T25 flasks in cDMEM or 50:50 cDMEM and WT CM or  
496 CATT<sub>7</sub> CM for 72 hr. Cells were trypsinised and stained with ethidium bromide/ acridine  
497 orange and counted on a haemocytometer. MIF inhibitor SCD-19 ( $100 \mu\text{M}$ ) was used to  
498 determine MIF specificity. In such cases, conditioned media was pre-incubated with SCD-19  
499 1 hr before the expansion assay.

## 500 **Intracellular Staining of COX-2 and IDO**

501 MSCs were seeded at  $1 \times 10^5$  cells per well in 6 well plates. MSCs were stimulated with  
502 recombinant human IFN $\gamma$  at low ( $5\text{ng}/\text{ml}$ ) or high ( $40\text{ng}/\text{ml}$ ) concentrations, TNF $\alpha$  ( $5\text{-}10\text{ng}/\text{ml}$ )

503 (PeproTech, London, UK), recombinant human MIF (1ng/ml) (provided by Rick Bucala, Yale)  
504 or endogenous MIF (CATT<sub>7</sub> CM) for 24 hr. Cells were prepared for intracellular staining using  
505 the Intracellular FoxP3 kit as per manufacturer's instructions. Cells were stained with COX-2  
506 (PE) or IDO (APC) (BD Pharmingen, San Diego, CA, USA) for 45 min. Cells were then  
507 washed in flow cytometry staining buffer and acquired using the Attune Nxt Flow Cytometer.

#### 508 **Surface Staining of CD74**

509 MSCs were seeded at  $1 \times 10^5$  cells per well in 6 well plates. MSCs were stimulated with  
510 recombinant human IFN $\gamma$  (5ng/ml) (PeproTech, London, UK), recombinant human MIF (1, 10  
511 or 100ng/ml) or endogenous MIF (CATT<sub>7</sub> CM) for 24 hr. Cells were stained with CD74 (PE)  
512 (BD Pharmingen, San Diego, CA, USA) for 45 min. Cells were then washed in flow cytometry  
513 staining buffer and acquired using the Attune Nxt Flow Cytometer.

#### 514 **T Cell Suppression assay**

515 Human PBMCs were isolated from buffy packs (Irish Blood Transfusion Service), by Ficoll  
516 density gradient centrifugation.  $5 \times 10^4$  Carboxyfluorescein succinimidyl ester (CFSE) labelled  
517 PBMC were co-cultured (ThermoFisher Scientific, Eugene, OR, USA) with BM-MSC in a  
518 1:20 ratio ( $2.5 \times 10^3$  cells/well). 24 hr prior to co-culture, BM-MSCs were incubated with  
519 CATT<sub>7</sub> CM or CATT<sub>7</sub> CM + SCD-19 (100  $\mu$ M). After 24 hr, BM-MSCs were washed with  
520 PBS before adding the PBMCs. Activation and expansion of human T cells was carried out  
521 using ImmunoCult<sup>TM</sup> human CD3/CD28 T cell activator antibody mix (STEMCELL  
522 Technologies, Cambridge, UK). After 4 days, PBMCs were harvested and the frequency (%)  
523 and number of proliferating CD3<sup>+</sup> T cells were analysed by flow cytometry (Attune Nxt Flow  
524 Cytometer).

#### 525 **Statistical Analysis**

526 Mice were randomised. Observers assessing end-points were blinded to group assignment.  
527 Data for individual animals and independent experiments are presented as individual symbols.  
528 All data are presented as mean  $\pm$  SEM. Results of two or more groups were compared by one-  
529 way analysis of variance (ANOVA) followed by the *post-hoc* Tukey's multiple comparison  
530 test. GraphPad Prism (GraphPad Software Inc, San Diego, CA, USA) was used for all statistical  
531 analyses.

**532 Data Availability Statement**

533 The data that support the findings of this study are available on request from the corresponding  
534 author.

**535 Acknowledgements**

536 This research was supported by an Irish Research Council Laureate Award to KE  
537 (IRCLA/2017/288). This publication has emanated from research supported in part by a  
538 research grant from Science Foundation Ireland (SFI) under grant number 12/RI/2346 (2); an  
539 infrastructure award supporting the CryoViz and SFI grant number 16/RI/3399; an  
540 infrastructure award supporting the Attune Nxt. We would like to thank Deirdre Daly, Gillian  
541 O'Meara and Shannon Grellan for their exceptional care of our animals used in this study.

**542 Author's Contributions**

543 IJH performed research, data analysis, study design and wrote the manuscript. HD performed  
544 research, data analysis, study design and wrote the manuscript. CT & TS performed research  
545 and data analysis; DJW, SRE & CCDS contributed to study design and data analysis. SCD &  
546 MEA provided reagents, contributed to study design and data analysis. KE designed and  
547 supervised the study and wrote the manuscript. All authors approved the final manuscript.

**548 Declaration of Interest**

549 The authors declare no conflict of interest.

**550 Keywords**

551 Mesenchymal Stromal Cells, House Dust Mite, Allergic Asthma, Macrophage Migration  
552 Inhibitory Factor, Cyclooxygenase

**553 References**

- 554 1. Sverrild A, Hansen S, Hvidtfeldt M, Clausson CM, Cozzolino O, Cerps S, Uller L, Backer  
555 V, Erjefält J, Porsbjerg C. The effect of tezepelumab on airway hyperresponsiveness to  
556 mannitol in asthma (UPSTREAM). *Eur Respir J.* 2022 Jan;59(1):2101296.
- 557 2. Bleecker ER, FitzGerald JM, Chanez P, Papi A, Weinstein SF, Barker P, Sproule S,  
558 Gilmartin G, Aurivillius M, Werkström V, et al. Efficacy and safety of benralizumab for  
559 patients with severe asthma uncontrolled with high-dosage inhaled corticosteroids and

- 560 long-acting  $\beta$ 2-agonists (SIROCCO): a randomised, multicentre, placebo-controlled  
561 phase 3 trial. *Lancet Lond Engl.* 2016 Oct 29;388(10056):2115–27.
- 562 3. Corren J, Castro M, O’Riordan T, Hanania NA, Pavord ID, Quirce S, Chipps BE, Wenzel  
563 SE, Thangavelu K, Rice MS, et al. Dupilumab efficacy in patients with uncontrolled,  
564 moderate-to-severe allergic asthma. *J Allergy Clin Immunol Pract.* 2020 Feb;8(2):516–  
565 26.
- 566 4. Ortega HG, Yancey SW, Mayer B, Gunsoy NB, Keene ON, Bleecker ER, Brightling CE,  
567 Pavord ID. Severe eosinophilic asthma treated with mepolizumab stratified by baseline  
568 eosinophil thresholds: a secondary analysis of the DREAM and MENSA studies. *Lancet*  
569 *Respir Med.* 2016 Jul 1;4(7):549–56.
- 570 5. Chan R, Lipworth B. Efficacy of biologic therapy on airway hyperresponsiveness in  
571 asthma. *Ann Allergy Asthma Immunol Off Publ Am Coll Allergy Asthma Immunol.* 2023  
572 Feb 23;S1081-1206(23)00121-7.
- 573 6. Goodwin M, Sueblinvong V, Eisenhauer P, Ziats NP, LeClair L, Poynter ME, Steele C,  
574 Rincon M, Weiss DJ. Bone marrow-derived mesenchymal stromal cells inhibit Th2-  
575 mediated allergic airways inflammation in mice. *Stem Cells Dayt Ohio.* 2011  
576 Jul;29(7):1137–48.
- 577 7. Abreu SC, Antunes MA, de Castro JC, de Oliveira MV, Bandeira E, Ornellas DS, Diaz  
578 BL, Morales MM, Xisto DG, Rocco PRM. Bone marrow-derived mononuclear cells vs.  
579 mesenchymal stromal cells in experimental allergic asthma. *Respir Physiol Neurobiol.*  
580 2013 Jun 15;187(2):190–8.
- 581 8. Choi JY, Hur J, Jeon S, Jung CK, Rhee CK. Effects of human adipose tissue- and bone  
582 marrow-derived mesenchymal stem cells on airway inflammation and remodeling in a  
583 murine model of chronic asthma. *Sci Rep.* 2022 Jul 14;12(1):12032.
- 584 9. Dai R, Yu Y, Yan G, Hou X, Ni Y, Shi G. Intratracheal administration of adipose derived  
585 mesenchymal stem cells alleviates chronic asthma in a mouse model. *BMC Pulm Med.*  
586 2018 Aug 8;18(1):131.
- 587 10. de Castro LL, Xisto DG, Kitoko JZ, Cruz FF, Olsen PC, Redondo PAG, Ferreira TPT,  
588 Weiss DJ, Martins MA, Morales MM, et al. Human adipose tissue mesenchymal stromal  
589 cells and their extracellular vesicles act differentially on lung mechanics and  
590 inflammation in experimental allergic asthma. *Stem Cell Res Ther.* 2017 24;8(1):151.
- 591 11. Hur J, Kang JY, Kim YK, Lee SY, Jeon S, Kim Y, Jung CK, Rhee CK. Evaluation of  
592 human MSCs treatment frequency on airway inflammation in a mouse model of acute  
593 asthma. *J Korean Med Sci.* 2020 May 12;35(23):e188.
- 594 12. Mathias LJ, Khong SML, Spyroglou L, Payne NL, Siatskas C, Thorburn AN, Boyd RL,  
595 Heng TSP. Alveolar macrophages are critical for the inhibition of allergic asthma by  
596 mesenchymal stromal cells. *J Immunol Baltim Md 1950.* 2013 Dec 15;191(12):5914–24.
- 597 13. Ou-Yang HF, Huang Y, Hu XB, Wu CG. Suppression of allergic airway inflammation in  
598 a mouse model of asthma by exogenous mesenchymal stem cells. *Exp Biol Med*  
599 *Maywood NJ.* 2011 Dec;236(12):1461–7.

- 600 14. Royce SG, Mao W, Lim R, Kelly K, Samuel CS. iPSC- and mesenchymoangioblast-  
601 derived mesenchymal stem cells provide greater protection against experimental chronic  
602 allergic airways disease compared with a clinically used corticosteroid. *FASEB J Off Publ*  
603 *Fed Am Soc Exp Biol.* 2019 May;33(5):6402–11.
- 604 15. Royce SG, Rele S, Broughton BRS, Kelly K, Samuel CS. Intranasal administration of  
605 mesenchymoangioblast-derived mesenchymal stem cells abrogates airway fibrosis and  
606 airway hyperresponsiveness associated with chronic allergic airways disease. *FASEB J.*  
607 2017;31(9):4168–78.
- 608 16. Song X, Xie S, Lu K, Wang C. Mesenchymal stem cells alleviate experimental asthma by  
609 inducing polarization of alveolar macrophages. *Inflammation.* 2015 Apr;38(2):485–92.
- 610 17. Zhong H, Fan XL, Fang SB, Lin YD, Wen W, Fu QL. Human pluripotent stem cell-  
611 derived mesenchymal stem cells prevent chronic allergic airway inflammation via TGF-  
612  $\beta$ 1-Smad2/Smad3 signaling pathway in mice. *Mol Immunol.* 2019 May 1;109:51–7.
- 613 18. Abreu SC, Xisto DG, de Oliveira TB, Blanco NG, de Castro LL, Kitoko JZ, Olsen PC,  
614 Lopes-Pacheco M, Morales MM, Weiss DJ, et al. Serum from asthmatic mice potentiates  
615 the therapeutic effects of mesenchymal stromal cells in experimental allergic asthma.  
616 *Stem Cells Transl Med.* 2019 Mar;8(3):301–12.
- 617 19. Abreu SC, Lopes-Pacheco M, da Silva AL, Xisto DG, de Oliveira TB, Kitoko JZ, de  
618 Castro LL, Amorim NR, Martins V, Silva LHA, et al. Eicosapentaenoic acid enhances  
619 the effects of mesenchymal stromal cell therapy in experimental allergic asthma. *Front*  
620 *Immunol.* 2018;9:1147.
- 621 20. Braza F, Dirou S, Forest V, Sauzeau V, Hassoun D, Chesné J, Cheminant-Muller MA,  
622 Sagan C, Magnan A, Lemarchand P. Mesenchymal stem cells induce suppressive  
623 macrophages through phagocytosis in a mouse model of asthma. *STEM CELLS.*  
624 2016;34(7):1836–45.
- 625 21. Castro LL, Kitoko JZ, Xisto DG, Olsen PC, Guedes HLM, Morales MM, Lopes-Pacheco  
626 M, Cruz FF, Rocco PRM. Multiple doses of adipose tissue-derived mesenchymal stromal  
627 cells induce immunosuppression in experimental asthma. *Stem Cells Transl Med.* 2020  
628 Feb;9(2):250–60.
- 629 22. Duong KM, Arikatt J, Ullah MA, Lynch JP, Zhang V, Atkinson K, Sly PD, Phipps S.  
630 Immunomodulation of airway epithelium cell activation by mesenchymal stromal cells  
631 ameliorates house dust mite-induced airway inflammation in mice. *Am J Respir Cell Mol*  
632 *Biol.* 2015 Nov;53(5):615–24.
- 633 23. Kitoko JZ, Castro LL de, Nascimento AP, Abreu SC, Cruz FF, Arantes AC, Xisto DG,  
634 Martins MA, Morales MM, Rocco PRM, et al. Therapeutic administration of bone  
635 marrow-derived mesenchymal stromal cells reduces airway inflammation without up-  
636 regulating Tregs in experimental asthma. *Clin Exp Allergy.* 2018;48(2):205–16.
- 637 24. Shin JW, Ryu S, Ham J, Jung K, Lee S, Chung DH, Kang HR, Kim HY. Mesenchymal  
638 stem cells suppress severe asthma by directly regulating Th2 cells and type 2 innate  
639 lymphoid cells. *Mol Cells.* 2021 Aug 31;44(8):580–90.



- 640 25. Cruz FF, Borg ZD, Goodwin M, Sokocevic D, Wagner DE, Coffey A, Antunes M,  
641 Robinson KL, Mitsialis SA, Kourembanas S, et al. Systemic administration of human  
642 bone marrow-derived mesenchymal stromal cell extracellular vesicles ameliorates  
643 aspergillus hyphal extract-induced allergic airway inflammation in immunocompetent  
644 mice. *Stem Cells Transl Med.* 2015 Nov;4(11):1302–16.
- 645 26. Lathrop MJ, Brooks EM, Bonenfant NR, Sokocevic D, Borg ZD, Goodwin M, Loi R,  
646 Cruz F, Dunaway CW, Steele C, et al. Mesenchymal stromal cells mediate *Aspergillus*  
647 hyphal extract-induced allergic airway inflammation by inhibition of the Th17 signaling  
648 pathway. *Stem Cells Transl Med.* 2014 Feb;3(2):194–205.
- 649 27. Abreu SC, Antunes MA, Xisto DG, Cruz FF, Branco VC, Bandeira E, Zola Kitoko J, de  
650 Araújo AF, Dellatorre-Teixeira L, Olsen PC, et al. Bone marrow, adipose, and lung tissue-  
651 derived murine mesenchymal stromal cells release different mediators and differentially  
652 affect airway and lung parenchyma in experimental asthma. *Stem Cells Transl Med.* 2017  
653 Jun;6(6):1557–67.
- 654 28. Mariñas-Pardo L, Mirones I, Amor-Carro Ó, Fraga-Iriso R, Lema-Costa B, Cubillo I,  
655 Rodríguez Milla MÁ, García-Castro J, Ramos-Barbón D. Mesenchymal stem cells  
656 regulate airway contractile tissue remodeling in murine experimental asthma. *Allergy.*  
657 2014 Jun;69(6):730–40.
- 658 29. Dunbar H, Weiss DJ, Rolandsson Enes S, Laffey JG, English K. The inflammatory lung  
659 microenvironment; a key mediator in MSC licensing. *Cells.* 2021 Nov 2;10(11):2982.
- 660 30. Liu J, Gao J, Liang Z, Gao C, Niu Q, Wu F, Zhang L. Mesenchymal stem cells and their  
661 microenvironment. *Stem Cell Res Ther.* 2022 Aug 20;13(1):429.
- 662 31. Sudres M, Norol F, Trenado A, Grégoire S, Charlotte F, Levacher B, Lataillade JJ, Bourin  
663 P, Holy X, Vernant JP, et al. Bone marrow mesenchymal stem cells suppress lymphocyte  
664 proliferation in vitro but fail to prevent graft-versus-host disease in mice. *J Immunol*  
665 *Baltim Md* 1950. 2006 Jun 15;176(12):7761–7.
- 666 32. Dorronsoro A, Ferrin I, Salcedo JM, Jakobsson E, Fernández-Rueda J, Lang V, Sepulveda  
667 P, Fechter K, Pennington D, Trigueros C. Human mesenchymal stromal cells modulate  
668 T-cell responses through TNF- $\alpha$ -mediated activation of NF- $\kappa$ B. *Eur J Immunol.* 2014  
669 Feb;44(2):480–8.
- 670 33. Tobin LM, Healy ME, English K, Mahon BP. Human mesenchymal stem cells suppress  
671 donor CD4(+) T cell proliferation and reduce pathology in a humanized mouse model of  
672 acute graft-versus-host disease. *Clin Exp Immunol.* 2013 May;172(2):333–48.
- 673 34. Weiss DJ, English K, Krasnodembskaya A, Isaza-Correa JM, Hawthorne IJ, Mahon BP.  
674 The necrobiology of mesenchymal stromal cells affects therapeutic efficacy. *Front*  
675 *Immunol.* 2019;10:1228.
- 676 35. Islam D, Huang Y, Fanelli V, Delsedime L, Wu S, Khang J, Han B, Grassi A, Li M, Xu  
677 Y, et al. Identification and modulation of microenvironment is crucial for effective  
678 mesenchymal stromal cell therapy in acute lung injury. *Am J Respir Crit Care Med.* 2019  
679 May 15;199(10):1214–24.

- 680 36. Ankrum JA, Ong JF, Karp JM. Mesenchymal stem cells: immune evasive, not immune  
681 privileged. *Nat Biotechnol.* 2014 Mar;32(3):252–60.
- 682 37. Mathew SA, Chandravanshi B, Bhonde R. Hypoxia primed placental mesenchymal stem  
683 cells for wound healing. *Life Sci.* 2017 Aug 1;182:85–92.
- 684 38. Roemeling-van Rhijn M, Mensah FKF, Korevaar SS, Leijns MJ, van Osch GJVM,  
685 Ijzermans JNM, Betjes MGH, Baan CC, Weimar W, Hoogduijn MJ. Effects of hypoxia  
686 on the immunomodulatory properties of adipose tissue-derived mesenchymal stem cells.  
687 *Front Immunol.* 2013;4:203.
- 688 39. Carty F, Dunbar H, Hawthorne IJ, Ting AE, Stubblefield SR, Van't Hof W, English K.  
689 IFN- $\gamma$  and PPAR $\delta$  influence the efficacy and retention of multipotent adult progenitor  
690 cells in graft vs host disease. *Stem Cells Transl Med.* 2021 Nov;10(11):1561–74.
- 691 40. Corbett JM, Hawthorne I, Dunbar H, Coulter I, Chonghaile MN, Flynn CM, English K.  
692 Cyclosporine A and IFN $\gamma$  licencing enhances human mesenchymal stromal cell potency  
693 in a humanised mouse model of acute graft versus host disease. *Stem Cell Res Ther.* 2021  
694 Apr 14;12(1):238.
- 695 41. Silva JD, Lopes-Pacheco M, de Castro LL, Kitoko JZ, Trivelin SA, Amorim NR,  
696 Capelozzi VL, Morales MM, Gutfilen B, de Souza SAL, et al. Eicosapentaenoic acid  
697 potentiates the therapeutic effects of adipose tissue-derived mesenchymal stromal cells  
698 on lung and distal organ injury in experimental sepsis. *Stem Cell Res Ther.* 2019  
699 23;10(1):264.
- 700 42. Bustos ML, Huleihel L, Meyer EM, Donnenberg AD, Donnenberg VS, Sciruba JD, Mroz  
701 L, McVerry BJ, Ellis BM, Kaminski N, et al. Activation of human mesenchymal stem  
702 cells impacts their therapeutic abilities in lung injury by increasing interleukin (IL)-10  
703 and IL-1RN levels. *Stem Cells Transl Med.* 2013 Nov;2(11):884–95.
- 704 43. Rolandsson Enes S, Hampton TH, Barua J, McKenna DH, Dos Santos CC, Amiel E,  
705 Ashare A, Liu KD, Krasnodembskaya AD, English K, et al. Healthy versus inflamed lung  
706 environments differentially affect mesenchymal stromal cells. *Eur Respir J.* 2021  
707 Oct;58(4):2004149.
- 708 44. Abreu SC, Hampton TH, Hoffman E, Dearborn J, Ashare A, Singh Sidhu K, Matthews  
709 DE, McKenna DH, Amiel E, Barua J, et al. Differential effects of the cystic fibrosis lung  
710 inflammatory environment on mesenchymal stromal cells. *Am J Physiol-Lung Cell Mol*  
711 *Physiol.* 2020 Sep 9;ajplung.00218.2020.
- 712 45. Bacher M, Metz CN, Calandra T, Mayer K, Chesney J, Lohoff M, Gemsa D, Donnelly T,  
713 Bucala R. An essential regulatory role for macrophage migration inhibitory factor in T-  
714 cell activation. *Proc Natl Acad Sci U S A.* 1996 Jul 23;93(15):7849–54.
- 715 46. Calandra T, Bernhagen J, Metz CN, Spiegel LA, Bacher M, Donnelly T, Cerami A,  
716 Bucala R. MIF as a glucocorticoid-induced modulator of cytokine production. *Nature.*  
717 1995 Sep 7;377(6544):68–71.
- 718 47. Calandra T, Bernhagen J, Mitchell RA, Bucala R. The macrophage is an important and  
719 previously unrecognized source of macrophage migration inhibitory factor. *J Exp Med.*  
720 1994 Jun 1;179(6):1895–902.

- 721 48. Donnelly SC, Haslett C, Reid PT, Grant IS, Wallace WA, Metz CN, Bruce LJ, Bucala R.  
722 Regulatory role for macrophage migration inhibitory factor in acute respiratory distress  
723 syndrome. *Nat Med.* 1997 Mar;3(3):320–3.
- 724 49. Das R, Moss JE, Robinson E, Roberts S, Levy R, Mizue Y, Leng L, McDonald C, Tigelaar  
725 RE, Herrick CA, et al. Role of macrophage migration inhibitory factor in the Th2 immune  
726 response to epicutaneous sensitization. *J Clin Immunol.* 2011 Aug;31(4):666–80.
- 727 50. Li R, Wang F, Wei J, Lin Y, Tang G, Rao L, Ma L, Xu Q, Wu J, Lv Q, et al. The role of  
728 macrophage migration inhibitory factor (MIF) in asthmatic airway remodeling. *Allergy  
729 Asthma Immunol Res.* 2021 Jan;13(1):88–105.
- 730 51. Magalhães ES, Mourao-Sa DS, Vieira-de-Abreu A, Figueiredo RT, Pires AL, Farias-  
731 Filho FA, Fonseca BPF, Viola JPB, Metz C, Martins MA, et al. Macrophage migration  
732 inhibitory factor is essential for allergic asthma but not for Th2 differentiation. *Eur J  
733 Immunol.* 2007 Apr;37(4):1097–106.
- 734 52. Mizue Y, Ghani S, Leng L, McDonald C, Kong P, Baugh J, Lane SJ, Craft J, Nishihira J,  
735 Donnelly SC, et al. Role for macrophage migration inhibitory factor in asthma. *Proc Natl  
736 Acad Sci U S A.* 2005 Oct 4;102(40):14410–5.
- 737 53. Allam VSRR, Pavlidis S, Liu G, Kermani NZ, Simpson J, To J, Donnelly S, Guo YK,  
738 Hansbro PM, Phipps S, et al. Macrophage migration inhibitory factor promotes  
739 glucocorticoid resistance of neutrophilic inflammation in a murine model of severe  
740 asthma. *Thorax.* 2022 Nov 7;thoraxjnl-2021-218555.
- 741 54. Amano T, Nishihira J, Miki I. Blockade of macrophage migration inhibitory factor (MIF)  
742 prevents the antigen-induced response in a murine model of allergic airway inflammation.  
743 *Inflamm Res Off J Eur Histamine Res Soc Al.* 2007 Jan;56(1):24–31.
- 744 55. Kobayashi M, Nasuhara Y, Kamachi A, Tanino Y, Betsuyaku T, Yamaguchi E, Nishihira  
745 J, Nishimura M. Role of macrophage migration inhibitory factor in ovalbumin-induced  
746 airway inflammation in rats. *Eur Respir J.* 2006 Apr;27(4):726–34.
- 747 56. Chen PF, Luo Y ling, Wang W, Wang J xin, Lai W yan, Hu S ming, Cheng KF, Al-Abed  
748 Y. ISO-1, a macrophage migration inhibitory factor antagonist, inhibits airway  
749 remodeling in a murine model of chronic asthma. *Mol Med Camb Mass.* 2010 Oct;16(9–  
750 10):400–8.
- 751 57. Awandare GA, Martinson JJ, Were T, Ouma C, Davenport GC, Ong’echa JM, Wang WK,  
752 Leng L, Ferrell RE, Bucala R, et al. Macrophage migration inhibitory factor (MIF)  
753 promoter polymorphisms and susceptibility to severe malarial anemia. *J Infect Dis.* 2009  
754 Aug 15;200(4):629–37.
- 755 58. Savva A, Brouwer MC, Roger T, Valls Serón M, Le Roy D, Ferwerda B, van der Ende  
756 A, Bochud PY, van de Beek D, Calandra T. Functional polymorphisms of macrophage  
757 migration inhibitory factor as predictors of morbidity and mortality of pneumococcal  
758 meningitis. *Proc Natl Acad Sci.* 2016 Mar 29;113(13):3597–602.
- 759 59. Benedek G, Meza-Romero R, Jordan K, Zhang Y, Nguyen H, Kent G, Li J, Siu E, Frazer  
760 J, Piecychna M, et al. MIF and D-DT are potential disease severity modifiers in male MS  
761 subjects. *Proc Natl Acad Sci U S A.* 2017 Oct 3;114(40):E8421–9.

- 762 60. Liu A, Bao F, Voravuthikunchai SP. CATT polymorphism in MIF gene promoter is  
763 closely related to human pulmonary tuberculosis in a southwestern China population. *Int*  
764 *J Immunopathol Pharmacol*. 2018 May 29;32:2058738418777108.
- 765 61. Shin JJ, Fan W, Par-Young J, Piecychna M, Leng L, Israni-Winger K, Qing H, Gu J, Zhao  
766 H, Schulz WL, et al. MIF is a common genetic determinant of COVID-19 symptomatic  
767 infection and severity. *QJM Mon J Assoc Physicians*. 2022 Oct 12;hcac234.
- 768 62. Dunbar H, Hawthorne IJ, Tunstead C, Armstrong ME, Donnelly SC, English K. Blockade  
769 of MIF biological activity ameliorates house dust mite-induced allergic airway  
770 inflammation in humanised MIF mice. *FASEB J*. 2023;37.
- 771 63. Lourenco S, Teixeira VH, Kalber T, Jose RJ, Floto RA, Janes SM. Macrophage Migration  
772 Inhibitory Factor - CXCR4 is the dominant chemotactic axis in human mesenchymal stem  
773 cell recruitment to tumors. *J Immunol Baltim Md 1950*. 2015 Apr 1;194(7):3463–74.
- 774 64. English K. Mechanisms of mesenchymal stromal cell immunomodulation. *Immunol Cell*  
775 *Biol*. 2013 Jan;91(1):19–26.
- 776 65. Chinnadurai R, Rajan D, Ng S, McCullough K, Arafat D, Waller EK, Anderson LJ,  
777 Gibson G, Galipeau J. Immune dysfunctionality of replicative senescent mesenchymal  
778 stromal cells is corrected by IFN $\gamma$  priming. *Blood Adv*. 2017 Apr 25;1(11):628–43.
- 779 66. Chinnadurai R, Copland IB, Garcia MA, Petersen CT, Lewis CN, Waller EK, Kirk AD,  
780 Galipeau J. Cryopreserved mesenchymal stromal cells are susceptible to T-cell mediated  
781 apoptosis which is partly rescued by IFN $\gamma$  licensing. *Stem Cells Dayt Ohio*. 2016  
782 Sep;34(9):2429–42.
- 783 67. Chinnadurai R, Bates PD, Kunugi KA, Nickel KP, DeWerd LA, Capitini CM, Galipeau  
784 J, Kimple RJ. Dichotomic potency of IFN $\gamma$  licensed allogeneic mesenchymal stromal cells  
785 in animal models of acute radiation syndrome and graft versus host disease. *Front*  
786 *Immunol [Internet]*. 2021 [cited 2023 Aug 28];12. Available from:  
787 <https://www.frontiersin.org/articles/10.3389/fimmu.2021.708950>
- 788 68. English K, Barry FP, Field-Corbett CP, Mahon BP. IFN- $\gamma$  and TNF- $\alpha$  differentially  
789 regulate immunomodulation by murine mesenchymal stem cells. *Immunol Lett*. 2007 Jun  
790 15;110(2):91–100.
- 791 69. Murphy N, Treacy O, Lynch K, Morcos M, Lohan P, Howard L, Fahy G, Griffin MD,  
792 Ryan AE, Ritter T. TNF- $\alpha$ /IL-1 $\beta$ -licensed mesenchymal stromal cells promote corneal  
793 allograft survival via myeloid cell-mediated induction of Foxp3+ regulatory T cells in the  
794 lung. *FASEB J Off Publ Fed Am Soc Exp Biol*. 2019 Aug;33(8):9404–21.
- 795 70. Gomes AO, Barbosa BF, Franco PS, Ribeiro M, Silva RJ, Gois PSG, Almeida KC,  
796 Angeloni MB, Castro AS, Guirelli PM, et al. Macrophage migration inhibitory factor  
797 (MIF) prevents maternal death, but contributes to poor fetal outcome during congenital  
798 toxoplasmosis. *Front Microbiol*. 2018;9:906.
- 799 71. Carli C, Metz CN, Al-Abed Y, Naccache PH, Akoum A. Up-regulation of  
800 cyclooxygenase-2 expression and prostaglandin E2 production in human endometriotic  
801 cells by macrophage migration inhibitory factor: involvement of novel kinase signaling  
802 pathways. *Endocrinology*. 2009 Jul;150(7):3128–37.

- 803 72. Mitchell RA, Liao H, Chesney J, Fingerle-Rowson G, Baugh J, David J, Bucala R.  
804 Macrophage migration inhibitory factor (MIF) sustains macrophage proinflammatory  
805 function by inhibiting p53: regulatory role in the innate immune response. *Proc Natl Acad*  
806 *Sci U S A*. 2002 Jan 8;99(1):345–50.
- 807 73. Li D, Han Y, Zhuang Y, Fu J, Liu H, Shi Q, Ju X. Overexpression of COX-2 but not  
808 indoleamine 2,3-dioxygenase-1 enhances the immunosuppressive ability of human  
809 umbilical cord-derived mesenchymal stem cells. *Int J Mol Med*. 2015 May;35(5):1309–  
810 16.
- 811 74. Guan Q, Ezzati P, Spicer V, Krokhin O, Wall D, Wilkins JA. Interferon  $\gamma$  induced  
812 compositional changes in human bone marrow derived mesenchymal stem/stromal cells.  
813 *Clin Proteomics*. 2017 Jul 6;14(1):26.
- 814 75. Lan H, Wang N, Chen Y, Wang X, Gong Y, Qi X, Luo Y, Yao F. Macrophage migration  
815 inhibitory factor (MIF) promotes rat airway muscle cell proliferation and migration  
816 mediated by ERK1/2 and FAK signaling. *Cell Biol Int*. 2018;42(1):75–83.
- 817 76. Ohta S, Misawa A, Fukaya R, Inoue S, Kanemura Y, Okano H, Kawakami Y, Toda M.  
818 Macrophage migration inhibitory factor (MIF) promotes cell survival and proliferation of  
819 neural stem/progenitor cells. *J Cell Sci*. 2012 Jul 1;125(Pt 13):3210–20.
- 820 77. Utispan K, Koontongkaew S. Macrophage migration inhibitory factor modulates  
821 proliferation, cell cycle, and apoptotic activity in head and neck cancer cell lines. *J Dent*  
822 *Sci*. 2021 Jan;16(1):342–8.
- 823 78. Kulesza A, Paczek L, Burdzinska A. The Role of COX-2 and PGE2 in the Regulation of  
824 Immunomodulation and Other Functions of Mesenchymal Stromal Cells. *Biomedicines*.  
825 2023 Feb;11(2):445.
- 826 79. Lin YD, Fan XL, Zhang H, Fang SB, Li CL, Deng MX, Qin ZL, Peng YQ, Zhang HY,  
827 Fu QL. The genes involved in asthma with the treatment of human embryonic stem cell-  
828 derived mesenchymal stem cells. *Mol Immunol*. 2018 Mar 1;95:47–55.
- 829 80. Fallon PG, Schwartz C. The high and lows of type 2 asthma and mouse models. *J Allergy*  
830 *Clin Immunol*. 2020 Feb 1;145(2):496–8.
- 831 81. Hass R, Kasper C, Böhm S, Jacobs R. Different populations and sources of human  
832 mesenchymal stem cells (MSC): A comparison of adult and neonatal tissue-derived MSC.  
833 *Cell Commun Signal CCS*. 2011 May 14;9:12.
- 834 82. Carty F, Corbett JM, Cunha JPMCM, Reading JL, Tree TIM, Ting AE, Stubblefield SR,  
835 English K. Multipotent adult progenitor cells suppress T Cell activation in in vivo models  
836 of homeostatic proliferation in a prostaglandin E2-dependent manner. *Front Immunol*.  
837 2018 Apr 23;9:645.
- 838 83. de Witte SFH, Merino AM, Franquesa M, Strini T, van Zogel JAA, Korevaar SS, Luk  
839 F, Gargsha M, O'Flynn L, Roy D, et al. Cytokine treatment optimises the  
840 immunotherapeutic effects of umbilical cord-derived MSC for treatment of inflammatory  
841 liver disease. *Stem Cell Res Ther*. 2017 Jun 8;8(1):140.

- 842 84. Baugh JA, Chitnis S, Donnelly SC, Monteiro J, Lin X, Plant BJ, Wolfe F, Gregersen PK,  
843 Bucala R. A functional promoter polymorphism in the macrophage migration inhibitory  
844 factor (MIF) gene associated with disease severity in rheumatoid arthritis. *Genes Immun.*  
845 2002 May;3(3):170–6.
- 846 85. Renner P, Roger T, Calandra T. Macrophage migration inhibitory factor: gene  
847 polymorphisms and susceptibility to inflammatory diseases. *Clin Infect Dis Off Publ*  
848 *Infect Dis Soc Am.* 2005 Nov 15;41 Suppl 7:S513-519.
- 849 86. Plant BJ, Gallagher CG, Bucala R, Baugh JA, Chappell S, Morgan L, O'Connor CM,  
850 Morgan K, Donnelly SC. Cystic fibrosis, disease severity, and a macrophage migration  
851 inhibitory factor polymorphism. *Am J Respir Crit Care Med.* 2005 Dec 1;172(11):1412–  
852 5.
- 853 87. Kim RL, Bang JY, Kim J, Mo Y, Kim Y, Lee CG, Elias JA, Kim HY, Kang HR.  
854 Mesenchymal stem cells exert their anti-asthmatic effects through macrophage  
855 modulation in a murine chronic asthma model. *Sci Rep.* 2022 Jun 13;12:9811.
- 856 88. Kabat M, Bobkov I, Kumar S, Grumet M. Trends in mesenchymal stem cell clinical trials  
857 2004-2018: Is efficacy optimal in a narrow dose range? *Stem Cells Transl Med.* 2019 Dec  
858 5;9(1):17–27.
- 859 89. Malaquias M a. S, Oyama LA, Jericó PC, Costa I, Padilha G, Nagashima S, Lopes-  
860 Pacheco M, Rebelatto CLK, Michelotto PV, Xisto DG, et al. Effects of mesenchymal  
861 stromal cells play a role the oxidant/antioxidant balance in a murine model of asthma.  
862 *Allergol Immunopathol (Madr).* 2018 Apr;46(2):136–43.
- 863 90. Kwak J, Choi SJ, Oh W, Yang YS, Jeon HB, Jeon ES. Cobalt chloride enhances the anti-  
864 inflammatory potency of human umbilical cord blood-derived mesenchymal stem cells  
865 through the ERK-HIF-1 $\alpha$ -microRNA-146a-mediated signaling pathway. *Stem Cells Int.*  
866 2018;2018:4978763.
- 867 91. Hong GH, Kwon HS, Lee KY, Ha EH, Moon KA, Kim SW, Oh W, Kim TB, Moon HB,  
868 Cho YS. hMSCs suppress neutrophil-dominant airway inflammation in a murine model  
869 of asthma. *Exp Mol Med.* 2017 27;49(1):e288.
- 870 92. Cruz FF, Borg ZD, Goodwin M, Coffey AL, Wagner DE, Rocco PRM, Weiss DJ.  
871 CD11b+ and Sca-1+ cells exert the main beneficial effects of systemically administered  
872 bone marrow-derived mononuclear cells in a murine model of mixed Th2/Th17 allergic  
873 airway inflammation. *STEM CELLS Transl Med.* 2016;5(4):488–99.
- 874 93. Zhilai Z, Biling M, Sujun Q, Chao D, Benchao S, Shuai H, Shun Y, Hui Z.  
875 Preconditioning in lowered oxygen enhances the therapeutic potential of human umbilical  
876 mesenchymal stem cells in a rat model of spinal cord injury. *Brain Res.* 2016 Jul  
877 1;1642:426–35.
- 878 94. Armitage J, Tan DBA, Troedson R, Young P, Lam KV, Shaw K, Sturm M, Weiss DJ,  
879 Moodley YP. Mesenchymal stromal cell infusion modulates systemic immunological  
880 responses in stable COPD patients: a phase I pilot study. *Eur Respir J.* 2018  
881 Mar;51(3):1702369.

- 882 95. Gholamrezanezhad A, Mirpour S, Bagheri M, Mohamadnejad M, Alimoghaddam K,  
883 Abdolazadeh L, Saghari M, Malekzadeh R. In vivo tracking of <sup>111</sup>In-oxine labeled  
884 mesenchymal stem cells following infusion in patients with advanced cirrhosis. *Nucl Med*  
885 *Biol.* 2011 Oct;38(7):961–7.
- 886 96. Sokal EM, Lombard CA, Roelants V, Najimi M, Varma S, Sargiacomo C, Ravau J, Mazza  
887 G, Jamar F, Versavau J, et al. Biodistribution of liver-derived mesenchymal stem cells  
888 after peripheral injection in a hemophilia A patient. *Transplantation.* 2017  
889 Aug;101(8):1845–51.
- 890 97. Koç ON, Gerson SL, Cooper BW, Dyhouse SM, Haynesworth SE, Caplan AI, Lazarus  
891 HM. Rapid hematopoietic recovery after coinfusion of autologous-blood stem cells and  
892 culture-expanded marrow mesenchymal stem cells in advanced breast cancer patients  
893 receiving high-dose chemotherapy. *J Clin Oncol Off J Am Soc Clin Oncol.* 2000  
894 Jan;18(2):307–16.
- 895 98. Sanchez-Diaz M, Quiñones-Vico MI, Sanabria de la Torre R, Montero-Vílchez T, Sierra-  
896 Sánchez A, Molina-Leyva A, Arias-Santiago S. Biodistribution of mesenchymal stromal  
897 cells after administration in animal models and humans: a systematic review. *J Clin Med.*  
898 2021 Jun 29;10(13):2925.
- 899 99. Kang I, Bucala R. The immunobiology of MIF: function, genetics and prospects for  
900 precision medicine. *Nat Rev Rheumatol.* 2019 Jul;15(7):427–37.
- 901 100. Farr L, Ghosh S, Moonah S. Role of MIF cytokine/CD74 receptor pathway in protecting  
902 against injury and promoting repair. *Front Immunol.* 2020;11:1273.
- 903 101. Bucala R, Shachar I. The integral role of CD74 in antigen presentation, MIF signal  
904 transduction, and B cell survival and homeostasis. *Mini Rev Med Chem.*  
905 2014;14(14):1132–8.
- 906 102. Imaoka M, Tanese K, Masugi Y, Hayashi M, Sakamoto M. Macrophage migration  
907 inhibitory factor-CD74 interaction regulates the expression of programmed cell death  
908 ligand 1 in melanoma cells. *Cancer Sci.* 2019 Jul;110(7):2273–83.
- 909 103. Klasen C, Ziehm T, Huber M, Asare Y, Kapurniotu A, Shachar I, Bernhagen J, El  
910 Bounkari O. LPS-mediated cell surface expression of CD74 promotes the proliferation of  
911 B cells in response to MIF. *Cell Signal.* 2018;46:32–42.
- 912 104. Soppert J, Kraemer S, Beckers C, Averdunk L, Möllmann J, Denecke B, Goetzenich A,  
913 Marx G, Bernhagen J, Stoppe C. Soluble CD74 reroutes MIF/CXCR4/AKT-mediated  
914 survival of cardiac myofibroblasts to necroptosis. *J Am Heart Assoc.* 2018  
915 04;7(17):e009384.
- 916 105. Flaster H, Bernhagen J, Calandra T, Bucala R. The macrophage migration inhibitory  
917 factor-glucocorticoid dyad: regulation of inflammation and immunity. *Mol Endocrinol.*  
918 2007 Jun 1;21(6):1267–80.
- 919 106. Sampey AV, Hall PH, Mitchell RA, Metz CN, Morand EF. Regulation of synoviocyte  
920 phospholipase A2 and cyclooxygenase 2 by macrophage migration inhibitory factor.  
921 *Arthritis Rheum.* 2001 Jun;44(6):1273–80.

- 922 107. Duffy MM, Pindjakova J, Hanley SA, McCarthy C, Weidhofer GA, Sweeney EM,  
 923 English K, Shaw G, Murphy JM, Barry FP, et al. Mesenchymal stem cell inhibition of T-  
 924 helper 17 cell- differentiation is triggered by cell–cell contact and mediated by  
 925 prostaglandin E2 via the EP4 receptor. *Eur J Immunol*. 2011;41(10):2840–51.
- 926 108. Cahill EF, Kennelly H, Carty F, Mahon BP, English K. Hepatocyte growth factor is  
 927 required for mesenchymal stromal cell protection against bleomycin-induced pulmonary  
 928 fibrosis. *Stem Cells Transl Med*. 2016 Oct;5(10):1307–18.
- 929 109. Sun L, Chen K, Jiang Z, Chen X, Ma J, Ma Q, Duan W. Indometacin inhibits the  
 930 proliferation and activation of human pancreatic stellate cells through the downregulation  
 931 of COX-2. *Oncol Rep*. 2018 May;39(5):2243–51.
- 932 110. Zhu W, Sun L, Zhao P, Liu Y, Zhang J, Zhang Y, Hong Y, Zhu Y, Lu Y, Zhao W, et al.  
 933 Macrophage migration inhibitory factor facilitates the therapeutic efficacy of  
 934 mesenchymal stem cells derived exosomes in acute myocardial infarction through  
 935 upregulating miR-133a-3p. *J Nanobiotechnology*. 2021 Feb 27;19:61.
- 936 111. Liu X, Li X, Zhu W, Zhang Y, Hong Y, Liang X, Fan B, Zhao H, He H, Zhang F.  
 937 Exosomes from mesenchymal stem cells overexpressing MIF enhance myocardial repair.  
 938 *J Cell Physiol*. 2020 Jan 20;
- 939 112. Zhang Y, Zhu W, He H, Fan B, Deng R, Hong Y, Liang X, Zhao H, Li X, Zhang F.  
 940 Macrophage migration inhibitory factor rejuvenates aged human mesenchymal stem cells  
 941 and improves myocardial repair. *Aging*. 2019 27;11(24):12641–60.
- 942 113. Zhang Y, Zhou Y, Chen S, Hu Y, Zhu Z, Wang Y, Du N, Song T, Yang Y, Guo A, et al.  
 943 Macrophage migration inhibitory factor facilitates prostaglandin E2 production of  
 944 astrocytes to tune inflammatory milieu following spinal cord injury. *J*  
 945 *Neuroinflammation*. 2019 Apr 13;16(1):85.
- 946 114. Fingerle-Rowson G, Petrenko O, Metz CN, Forsthuber TG, Mitchell R, Huss R, Moll U,  
 947 Müller W, Bucala R. The p53-dependent effects of macrophage migration inhibitory  
 948 factor revealed by gene targeting. *Proc Natl Acad Sci U S A*. 2003 Aug 5;100(16):9354–  
 949 9.
- 950 115. Cahill EF, Tobin LM, Carty F, Mahon BP, English K. Jagged-1 is required for the  
 951 expansion of CD4+ CD25+ FoxP3+ regulatory T cells and tolerogenic dendritic cells by  
 952 murine mesenchymal stromal cells. *Stem Cell Res Ther*. 2015 Mar 11;6(1):19.
- 953 116. Ehrentraut H, Clambey ET, McNamee EN, Brodsky KS, Ehrentraut SF, Poth JM, Riegel  
 954 AK, Westrich JA, Colgan SP, Eltzschig HK. CD73+ regulatory T cells contribute to  
 955 adenosine-mediated resolution of acute lung injury. *FASEB J Off Publ Fed Am Soc Exp*  
 956 *Biol*. 2013 Jun;27(6):2207–19.

957

958 **List of Figure Captions**



959 **Figure 1. Human BM-MSCs significantly reduce goblet cell metaplasia and collagen**  
 960 **deposition in CATT<sub>7</sub> mice challenged with HDM.** **A** PBS and HDM groups received PBS or  
 961 HDM i.n. 3 times a week for 3 consecutive weeks.  $1 \times 10^6$  human BM-MSCs were administered  
 962 i.v. to the HDM+MSC groups on day 14. Mice were sacrificed on day 21 (Schematic created  
 963 with BioRender.com). **B** Representative images of lung tissue from WT, CATT<sub>5</sub> and CATT<sub>7</sub>  
 964 mice stained with Periodic acid Schiff (PAS) at 20X magnification, scale bar = 20  $\mu$ m. Arrows  
 965 show examples of mucin-containing goblet cells. **C** Goblet cell hyperplasia was investigated  
 966 through the quantitation of PAS positive cells. **D** Representative images of lung tissue stained  
 967 with Masson's trichome at 4X magnification, scale bar = 200  $\mu$ m. **E** Quantitation of %  
 968 subepithelial collagen. Data are presented as mean  $\pm$  SEM; N=6 per group. Human BM-MSC  
 969 donors 001-177 and 003-310 were used (RoosterBio Inc., Frederick, MD, USA). Statistical  
 970 analysis was carried out using one-way ANOVA followed by the *post-hoc* Tukey's multiple  
 971 comparison test where \* $p < 0.05$ , \*\*\* $p < 0.001$ , \*\*\*\* $p < 0.0001$ , ns: non significant.

972

973 **Figure 2. Human BM-MSCs significantly reduce levels of Th2 cytokines in the BAL fluid**  
 974 **of CATT<sub>7</sub> mice challenged with HDM.** PBS and HDM groups received PBS or HDM i.n. 3  
 975 times a week for 3 consecutive weeks.  $1 \times 10^6$  human BM-MSCs were administered i.v. to the  
 976 HDM+MSC groups on day 14. BAL was performed 4 hr post final HDM challenge on day 18.  
 977 **A** Total cell count recovered from the BAL. **B** BAL fluid eosinophil count determined by  
 978 differential staining of cytopins. Cytokine levels of **C** IL-4 and **D** IL-13 in the BAL fluid  
 979 determined by ELISA. White bar: PBS; Grey bar: HDM; Blue bar: HDM+MSC. Data are  
 980 presented as mean  $\pm$  SEM; N=5-6 per group. Human BM-MSC donors 001-177 and 003-310  
 981 were used (RoosterBio Inc., Frederick, MD, USA). Statistical analysis was carried out using  
 982 one-way ANOVA. followed by the *post-hoc* Tukey's multiple comparison test where \* $p < 0.05$ ,  
 983 \*\* $p < 0.01$ , \*\*\* $p < 0.001$ , \*\*\*\* $p < 0.0001$ , ns: non significant.

984

985 **Figure 3. High levels of hMIF significantly enhance BM-MSC retention in a HDM model**  
 986 **of allergic asthma.** HDM was administered i.n. 3 times a week for 2 weeks. On day 14,  $1 \times 10^6$   
 987 Qtracker 625- labelled hMSCs were administered i.v. in WT, CATT<sub>5</sub> or CATT<sub>7</sub> mice. 24 hr  
 988 later the lungs were harvested, embedded in OCT compound and frozen at -80. Tissue blocks  
 989 were sectioned and imaged using the CryoViz<sup>TM</sup> (Bioinvision, Cleveland, OH, USA) imaging

990 system. 3D images show representative lung images from **A** WT, **B** CATT<sub>5</sub> and **C** CATT<sub>7</sub> mice  
 991 with detected MSCs shown in yellow. **D** Total number of MSCs detected in the lung and **E**  
 992 number of clusters were quantified using CryoViz™ Quantification software. Data are  
 993 presented as mean ± SEM; N=3 per group. Human BM-MSc donor 001-177 was used  
 994 (RoosterBio Inc., Frederick, MD, USA). Statistical analysis was carried out using one-way  
 995 ANOVA followed by the *post-hoc* Tukey's multiple comparison test where \*\*p<0.01.

996 **Figure 4. Influence of rhMIF licensing on MSC expression of immunomodulatory factors**  
 997 *in vitro*. **A-E** Gene expression of IDO, COX-2, PTGES, ICAM-1 and HGF by hBM-MSCs  
 998 after stimulation with recombinant human MIF (1ng/ml), human TNF $\alpha$  or human IFN $\gamma$  for  
 999 24hr. Data are presented as mean ± SEM and are representative of 3 independent experiments.  
 1000 Human BM-MSc donors 001-177, 003-310 and 003-307 were used (RoosterBio Inc.,  
 1001 Frederick, MD, USA). Statistical analysis was carried out using one-way ANOVA where  
 1002 \*p<0.05, \*\*p<0.01, \*\*\*\*p<0.0001, ns: non significant.

1003

1004 **Figure 5. CATT<sub>7</sub> MIF licensing enhances MSC expansion and immunosuppressive**  
 1005 **function *in vitro*.**

1006 **A** Schematic (created using Biorender.com) depicting the generation of CATT<sub>7</sub> MIF CM and  
 1007 experimental design. **B-E** Percentage or mean fluorescence intensity (MFI) of IDO or COX-2  
 1008 expression in human BM-MSCs measured by flow cytometry after cells were stimulated with  
 1009 CATT<sub>7</sub> MIF CM, human TNF $\alpha$  or human IFN $\gamma$  for 24hr. **F** Percentage expression and  
 1010 representative histogram plots of CD74 surface expression on human MSCs measured by flow  
 1011 cytometry after cells were stimulated with CATT<sub>7</sub> MIF CM and human IFN $\gamma$  for 24hr. **G-H**  
 1012 Relative gene expression of TSG-6 and PTGS2 by hBM-MSCs after cells were stimulated with  
 1013 endogenous human MIF (CATT<sub>7</sub> CM) and human TNF $\alpha$  for 6hr. **I-J** Licensing of MSCs with  
 1014 supernatants generated from BMDMs from CATT<sub>7</sub> HDM challenged mice enhances MSC  
 1015 suppression of **(I)** frequency (%) and **(J)** absolute number of CD3<sup>+</sup> T cells proliferating.  
 1016 Blockade of MIF using SCD-19 (100  $\mu$ M) in the BMDM supernatants 1 hr before addition to  
 1017 MSCs abrogates the enhanced effect of MIF on MSC suppression of T cell proliferation **(I-J)**.  
 1018 **K** Licensing of MSCs with CATT<sub>7</sub> MIF CM enhances MSC expansion *in vitro*. Addition of  
 1019 MIF inhibitor SCD-19 (100  $\mu$ M) to CATT<sub>7</sub> MIF CM 1 hr before MSC licensing prevents MIF  
 1020 enhanced MSC expansion. Data are presented as mean ± SEM and are representative of 3

1021 independent experiments. Human BM-MSC donors 001-177, 003-310 and 003-307 were used  
1022 (RoosterBio Inc., Frederick, MD, USA). Statistical analysis was carried out using a one-way  
1023 ANOVA or unpaired t test where \* $p < 0.05$ , \*\* $p < 0.01$ , \*\*\* $p < 0.001$ , \*\*\*\* $p < 0.0001$ , ns: non  
1024 significant.

1025

1026 **Figure 6. Titration of BM-MSC doses in CATT<sub>7</sub> mice challenged with HDM.** **A** To  
1027 determine the point where MSCs lose efficacy in CATT<sub>7</sub> mice, a range of doses were  
1028 administered on day 14. BAL was performed 4 hr post final HDM challenge on day 18  
1029 (Schematic created with BioRender.com). **B** Total cell count recovered from the BAL. **C**  
1030 Number of eosinophils obtained from the BAL fluid. Cytokine levels of **D** IL-4 and **E** IL-13 in  
1031 the BAL fluid determined by ELISA. Data are presented as mean  $\pm$  SEM; N=2-3 per group.  
1032 Human BM-MSC donors 001-177 and 003-310 were used (RoosterBio Inc., Frederick, MD,  
1033 USA). Statistical analysis was carried out using one-way ANOVA followed by the *post-hoc*  
1034 Tukey's multiple comparison test where \* $p < 0.05$ .

1035

1036 **Figure 7. MIF licensing restores MSC efficacy at low doses in CATT<sub>7</sub> mice.** **A**  $5 \times 10^4$  MSCs  
1037 were administered to HDM challenged CATT<sub>7</sub> mice on day 14. <sup>CATT7</sup>MSCs were licensed with  
1038 CATT<sub>7</sub> BMDM supernatant for 24 hr prior to i.v. administration. The control group <sup>KO</sup>MSCs  
1039 were generated by licensing MSCs with BMDM supernatant from MIF KO mice 24 hr prior to  
1040 i.v. administration. BAL was performed 4 hr post final HDM challenge on day 18 (Schematic  
1041 created with BioRender.com). **B** Total number of cells in the BAL were determined and  
1042 differential cell counts were performed on the collected cells to determine the numbers of **C**  
1043 eosinophils. Cytokine levels of **D** IL-4 and **E** IL-13 in the BAL fluid determined by ELISA.  
1044 Data are presented as mean  $\pm$  SEM; N=5-6 per group. Human BM-MSC donors 001-177 and  
1045 003-310 were used (RoosterBio Inc., Frederick, MD, USA). Statistical analysis was carried out  
1046 using one-way ANOVA followed by the *post-hoc* Tukey's multiple comparison test where  
1047 \* $p < 0.05$ .

1048

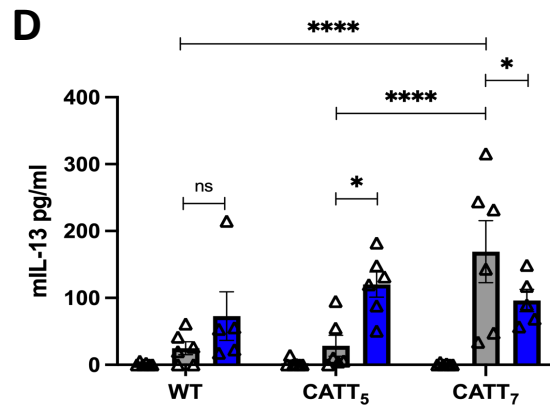
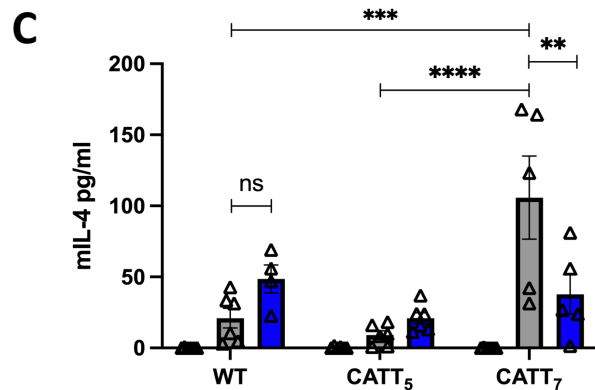
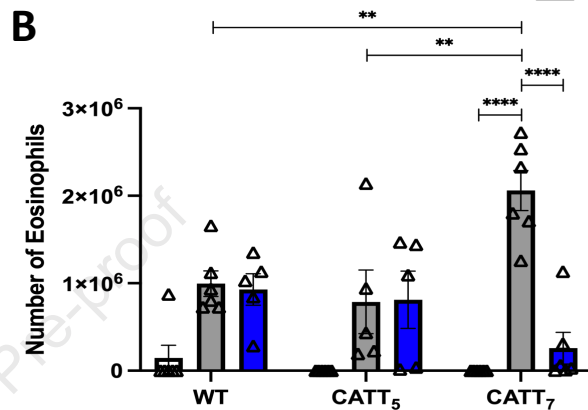
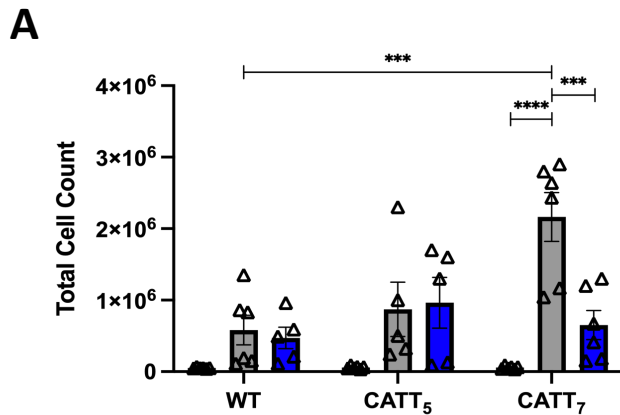
1049 **Figure 8. MIF-Licensed MSCs mediate their protective effects in HDM-induced allergic**  
1050 **airway inflammation in a CD74 and COX-2 dependent manner in CATT<sub>7</sub> mice.** **A**  $5 \times 10^4$

1051 MSCs were exposed to the COX-2 inhibitor indomethacin, an anti-CD74 neutralising antibody  
1052 or an isotype control antibody for 24 hr *in vitro*. All MSCs were licensed with CATT<sub>7</sub> BMDM  
1053 supernatant for 24 hr prior to i.v. administration. BAL was performed 4 hr post final HDM  
1054 challenge on day 18 (Schematic created with BioRender.com). **B** Total number of cells in the  
1055 BAL were determined and differential cell counts were performed on the collected cells to  
1056 determine the numbers of **C** eosinophils. Cytokine levels of **D** IL-4 and **E** IL-13 in the BAL  
1057 fluid determined by ELISA. Data are presented as mean  $\pm$  SEM; N=5-6 per group. Human  
1058 BM-MSC donors 001-177 and 003-310 were used (RoosterBio Inc., Frederick, MD, USA).  
1059 Statistical analysis was carried out using one-way ANOVA followed by the *post-hoc* Tukey's  
1060 multiple comparison test where \*p<0.

1061

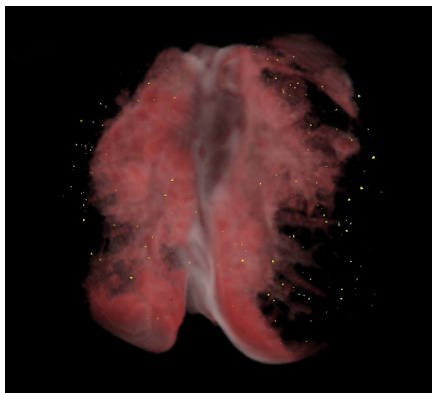
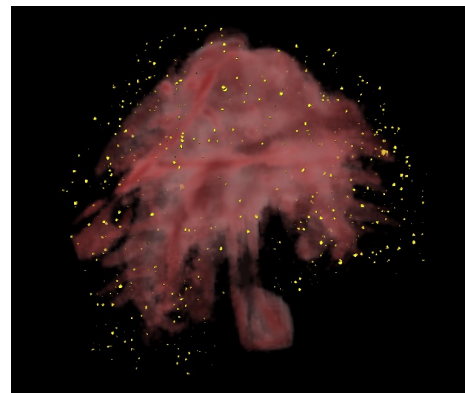


PBS  
 HDM  
 HDM + MSC

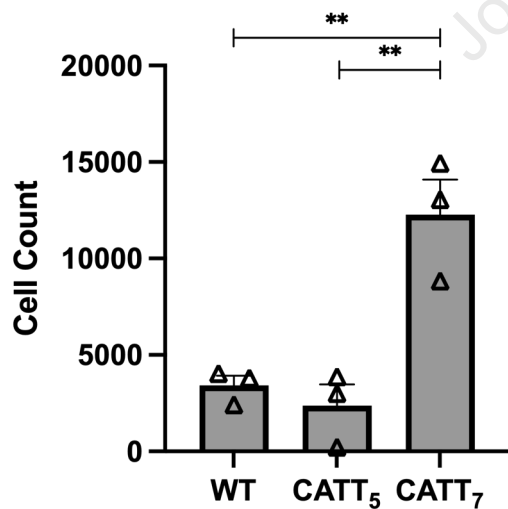


A

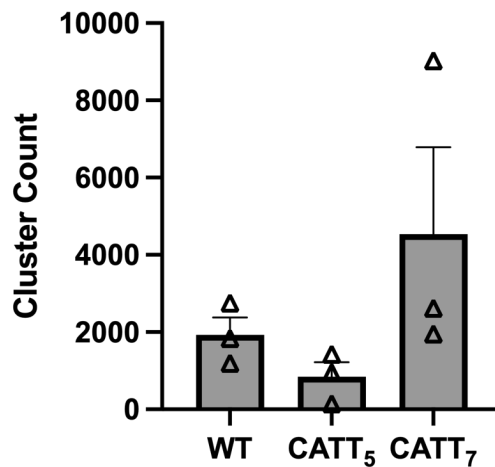
WT

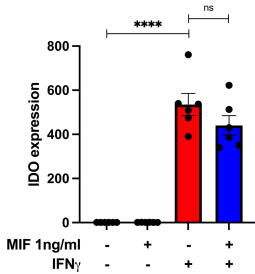
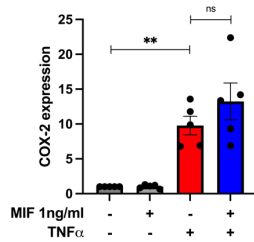
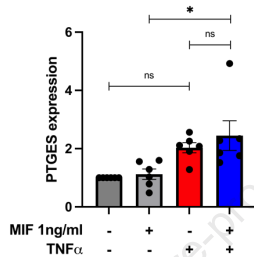
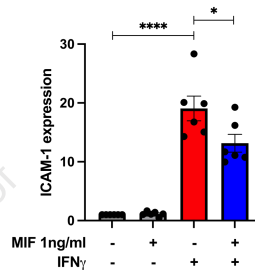
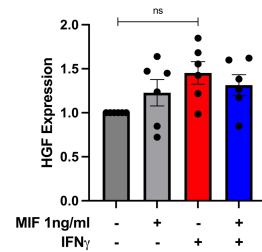
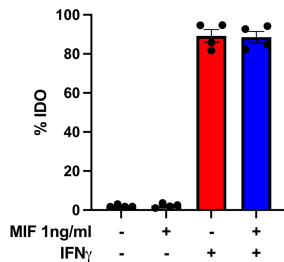
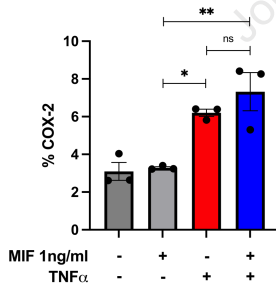
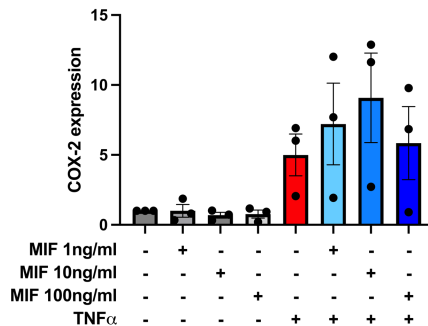
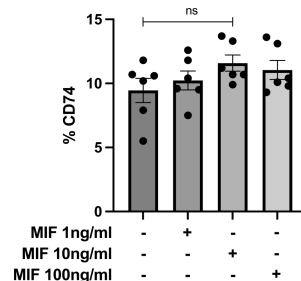
CATT<sub>5</sub>CATT<sub>7</sub>

D

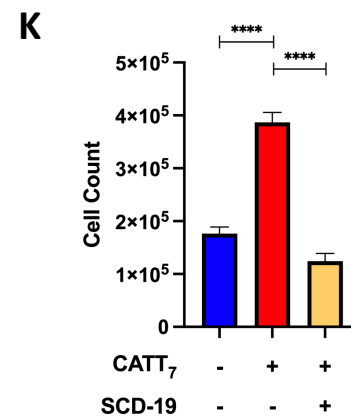
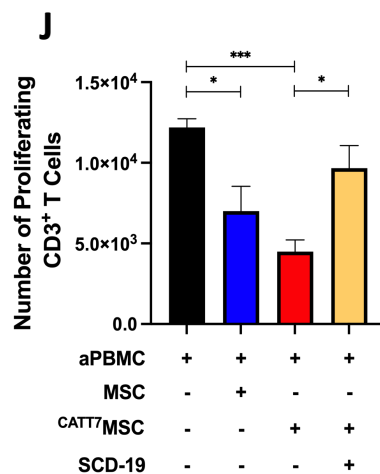
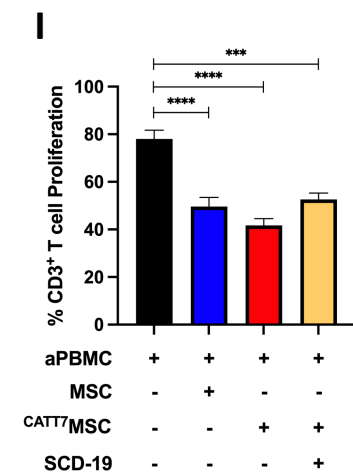
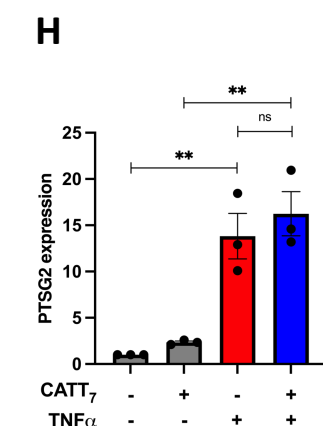
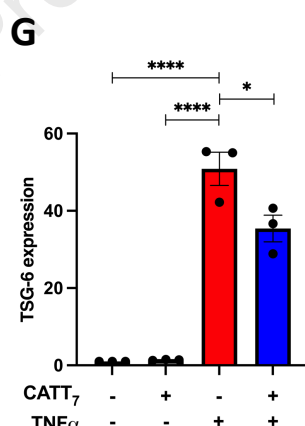
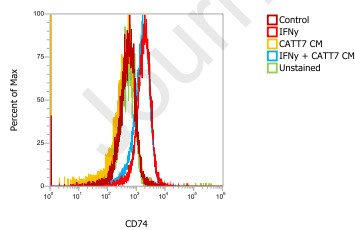
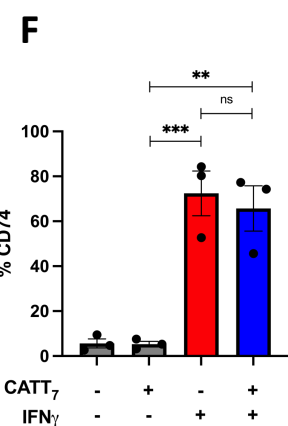
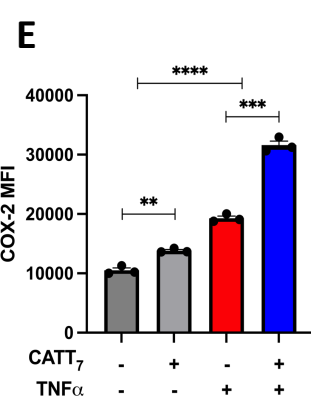
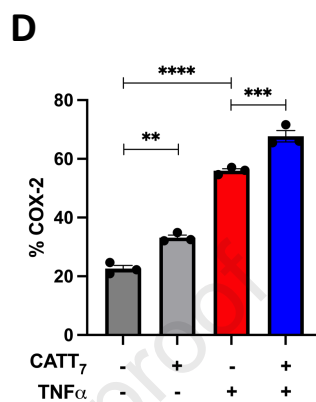
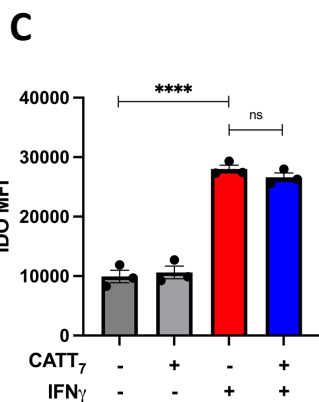
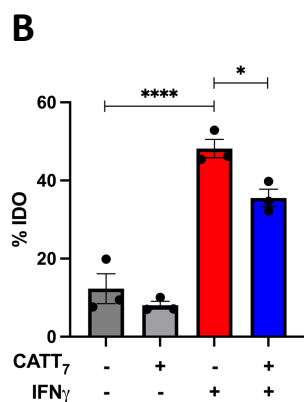
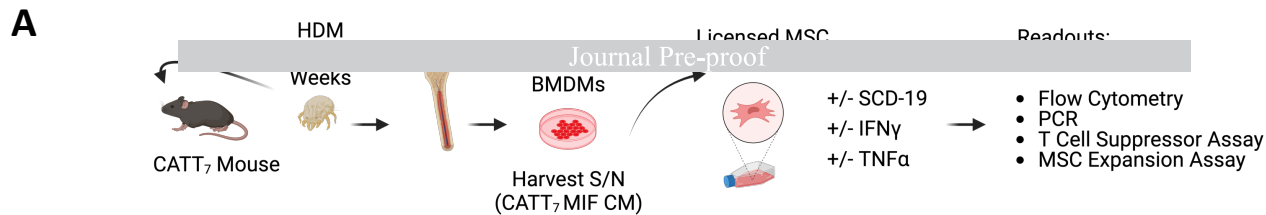


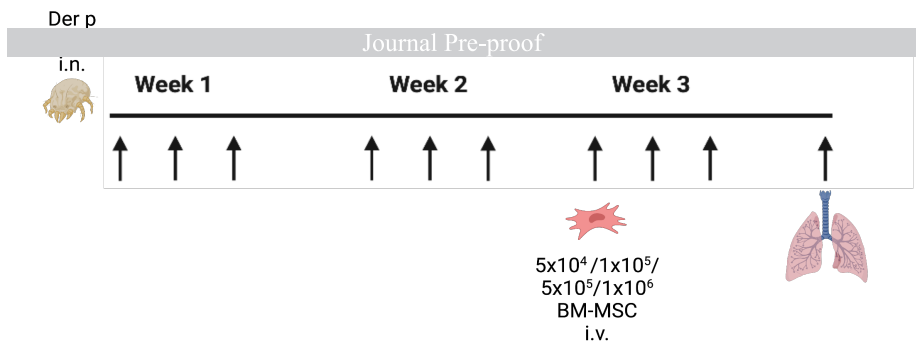
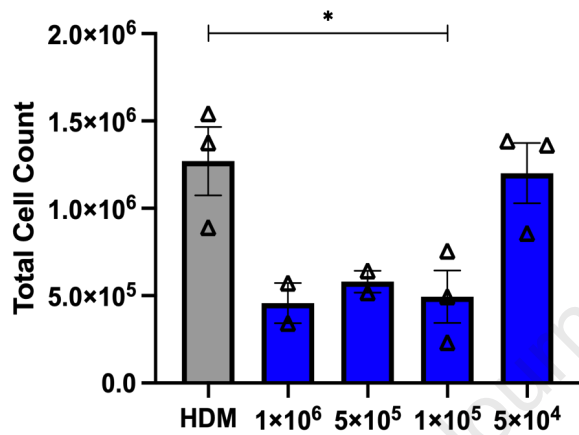
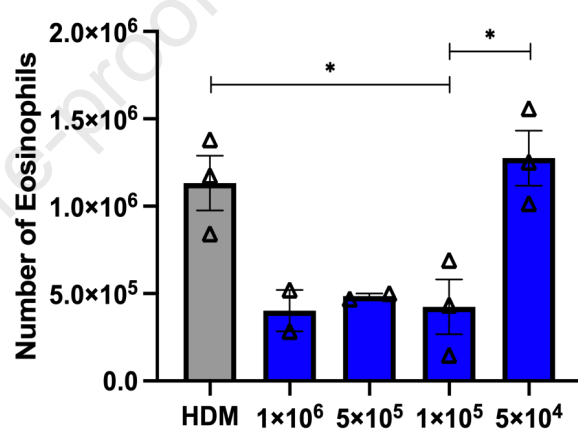
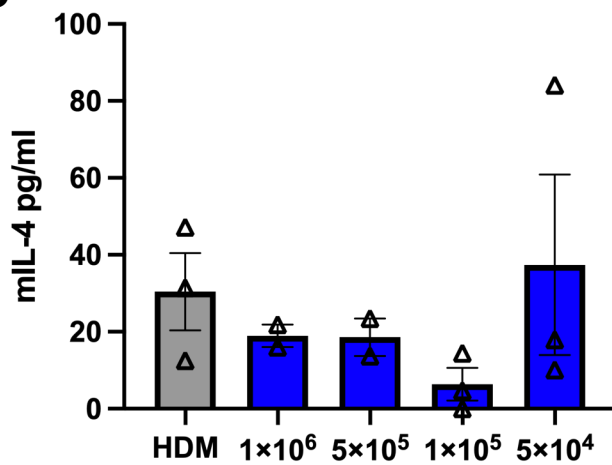
E



**A****B****C****D****E****F****G****H****I**





**A****B****C****D****E**